GIRMOS: Gemini Infrared Multi-Object Spectrograph

Science Cases

Document Number: GIRMOS.SCI.DOC.0001.C

Approvers List

Prepared by	Adam Muzzin, Alan McConnachie Project Scientist	Signature
Reviewed by	Suresh Sivanandam Principal Investigator	Signature
Approved by	Scott Christie Project Manager	Signature

Revisions

Revision	Change Description	Date
A	Initial Draft	2019-07-15
B	Release for Rebaseline Review	2021-01-08
C	New Draft with Imager Cases and updates to GNAO	2022-02-04

1. Table of Contents

1.1. Applicable Documents

Applicable Documents are those documents containing information that is considered binding in the context of this document. Unless otherwise specified, the latest version of the Applicable Document shall be used. In case of conflict between an Applicable Document and this document, this document shall take precedent.

	Document #	**Title**

1.2. Reference Documents

Reference documents are those documents that are included for information purposes only. They may provide additional background or context, but are non-binding in the context of this document.

	Document #	**Title**
	GIRMOS.SCI.0002	Science Requirements
	GIRMOS.SCI.0003	Concept of Operations
	GIRMOS.SYS.0002	Instrument Requirements

1.3. Acronyms/Abbreviations

Acronym	**Meaning**
AGN	Active Galactic Nuclei
AO	Adaptive Optics
DSFG	Dusty Star Forming Galaxies
FOV	Field of View
FWHM	Full-Width at Half-Maximum
GC	Globular Cluster
GIRMOS	Gemini Infrared Multi-Object Spectrograph
GST	GIRMOS Science Team

HST	Hubble Space Telescope
IFU	Integral field Unit
ISM	Interstellar Medium
IMBH	Intermediate-Mass Black Holes
LTAO	Laser Tomography Adaptive Optics
MOAO	Multi-Object Adaptive Optics
PI	Principal Investigator
RPS	Ram Pressure Stripping
SEMP	Systems Engineering Management Plan
SFR	Star Formation Rate
SMBH	Super Massive Black Hole
S/N	Signal-to-Noise Ratio
TBC	To Be Confirmed
TBD	To Be Determined

2. Purpose

The purpose of this document is to present an overview of the primary science cases driving the design requirements of the GIRMOS instrument. These science cases are likely to form a large component of the "first light" science performed by GIRMOS.

3. Scope

This document presents the GIRMOS Science Cases, which are a narrative description of the overall scientific goals of the instrument. The cases are contributed by the GIRMOS Science Team and members of the scientific community. Through the use of science cases, the astronomy community describes what they intend to study with GIRMOS, and why this is important, and how this instrument fits within the landscape of existing and planned capabilities at other observatories.

This document also captures the science requirements and that describe the minimum instrument capabilities which are needed to fulfill the observing parameters identified in each of the science cases. These key stakeholder expectations are expressed as Level 1 requirements in the Instrument Requirements Document. This flow-down of requirements is described fully in the GIRMOS Systems Engineering Management Plan (SEMP) [AD-01].

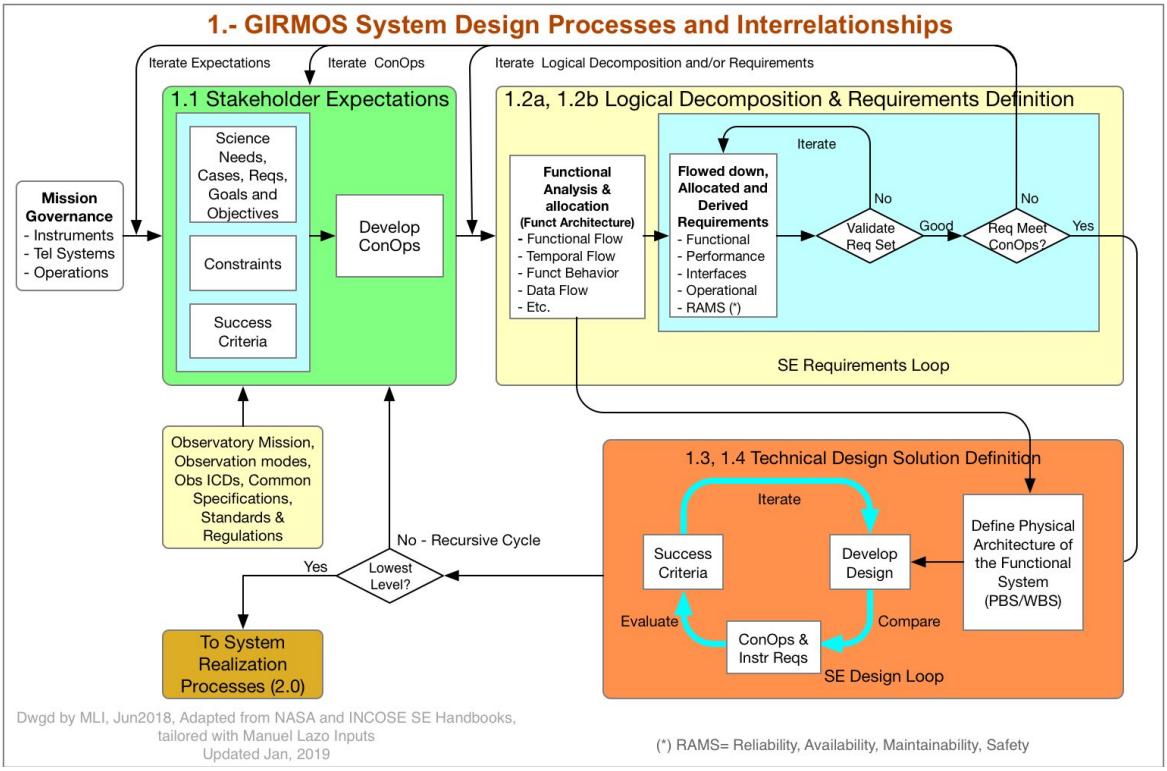

Figure 1: GIRMOS System Design Process

4. Project Structure

4.1. The Science Team

The GIRMOS Science Team is composed of members of physics and astronomy research institutions from around the world, however, the majority of members are located at Canadian Institutes. The mandate of the science team is to evaluate top-level science projects for the GIRMOS instrument and define the science requirements needed to fulfill those goals. The team also provides ongoing feasibility studies in collaboration with the instrument team during the design and fabrication phase. Our mandate is also to promote GIRMOS within the greater astronomical community. After commissioning, the GIRMOS science team will lead legacy programs on GIRMOS in order to cement the long-term impact of the instrument. The team will also direct the use of any guaranteed time observations given in exchange for the instrument.
Any and all full-time faculty, postdocs, and students working at a Canadian institute are welcome to become members of the GST. For such collaborators, appointment to the GST will be made by the approval of both the Instrument PI (Sivanandam) as well as the Project Scientist (Muzzin). Members outside of Canada are also welcome and can

become members through an appointment process. The current membership (as of March 2022) of the GIRMOS Science Team is:

- Suresh Sivanandam (University of Toronto)
- Adam Muzzin (York University)
- Alan McConnachie (NRC Herzberg)
- Roberto Abraham (University of Toronto)
- Masayuki Akiyama (Tohoku University)
- Dave Andersen (NRC Herzberg)
- Ray Carlberg (University of Toronto)
- Scott Chapman (Dalhousie University)
- Ivana Damjanov (St. Mary's University)
- Tim Davidge (NRC Herzberg)
- Sara Ellison (University of Victoria)
- Greg Fahlman (NRC Herzberg)
- Vincent Henault-Brunet (NRC Herzberg)
- Paul Hickson (NRC Herzberg)
- Masen Lamb (University of Toronto)
- Marie Lemoine-Busserolle (Gemini Observatory)
- Allison Man (University of Toronto)
- Trevor Mendel (Australian National University)
- Dae-Sik Moon (University of Toronto)
- Norm Murray (University of Toronto)
- Marcin Sawicki (St. Mary's University)
- Luc Simard (NRC Herzberg)
- Kim Venn (University of Victoria)
- Emily Wisnioski (Australian National University)
- Howard Yee (University of Toronto)

5. Infrared Multi-Object Spectroscopy using IFUs

5.1. Overview of Existing IFU Spectrographs

Many of the world's 8m-class telescopes employ IR IFU spectrographs as part of their instrument complement. The majority of these are single-object IFUs with AO capability. This includes SINFONI on the VLT (currently undergoing an upgrade and will be renamed ERIS upon re-commissioning), OSIRIS on Keck, and NIFS on Gemini. KMOS on VLT is also an NIR IFU, however, it is unique compared to these instruments in that it is (currently) the only multi-object NIR IFU (24 arms). Unlike the single-object IFUs, KMOS is currently not capable of running with AO. GIRMOS, with both AO capability and multi-object IFU capability will occupy a unique parameter space

amongst the current generation of NIR IFUs. GIRMOS is designed to be the first instrument capable of doing large IFU surveys with AO.

5.1.1. SINFONI/ERIS on VLT

5.1.1.1.Overview of SINFONI*

SINFONI is a near-infrared (1.1 -- 2.45 μm) IFU spectrograph fed by an AO module. The spectrograph operates with 4 gratings (J, H, K, H+K) providing a spectral resolution around 2000, 3000, 4000 in J, H & K respectively, and 1500 in H+K -- each wavelength band fitting fully on the 2048 pixels of the Hawaii 2RG (2k x 2k) detector in the dispersion direction. The SINFONI field of view on the sky is sliced into 32 slices/slitlets. The pre-slit optics allows 3 choices of the slice height. The choices are 250 mas, 100 mas and 25 mas, leading to field of views on the sky of 8"x8", 3"x3", and 0.8"x0.8" respectively. Each one of the 32 slitlets is imaged onto 64 pixels of the detector. Thus one obtains 64x32 spectra of the imaged region on the sky.

SINFONI can be used without adaptive optics guide stars -- the noAO mode -- in which case the AO module just acts as relay optics and the spatial resolution is dictated by the natural seeing. The full power of the instrument is, of course, achieved when a Natural Guide Star is available (NGS). For best correction, the star should be brighter than R ~ 11 mag. However, the AO can work (and will provide moderate improvement in image quality) with stars as faint as R ~ 17 mag in the best atmospheric conditions (good seeing and high coherence time or length).

* See http://www.eso.org/sci/facilities/paranal/instruments/sinfoni/overview.html

5.1.1.2. Science with SINFONI

SINFONI was first commissioned in June of 2004 (see Bonnet et al. 2004). It was offered for GO observations after Period 75 and was available until Period 103 (covering a span of 14 years). After period 103 it was removed from the telescope so that components could be reused in the ERIS upgrade. Over its 14-year lifetime SINFONI made considerable discoveries and contributions to multiple science fields. Perhaps its highest-impact results were from the SINS survey (e.g., Forster Schreiber et al. 2009; Genzel et al. 2011; Genzel et al. 2008) which was a primarily seeing-limited survey of ~80 galaxies at z ~ 2 (approximately 10 objects were observed with LGS AO). SINS identified the kinematic structure of high-redshift galaxies for the first time and showed that the majority are rotating disks, however, they typically have much more turbulence than lower-redshift galaxies. SINS also identified evidence for AGN driven winds in galaxies, a leading candidate for the feedback process that quenches star formation in galaxies. SINFONI's other major impact was high angular resolution observations of the Galactic centre which better refined models of the orbits of stars around the central black hole, and also caught several flaring events from Sagittarius A*. SINFONI also recently completed the SINS-zC-SINF survey, which performed LGS AO observations of

~30 galaxies at z = 2 (Forster Schreiber et al. 2019), now the largest sample of distant galaxies observed with AO. The forthcoming results of SINS-zc-SINF will clearly dictate future science directions for GIRMOS.

5.1.1.3. ERIS Upgrade

The Enhanced Resolution Imager and Spectrograph (ERIS) is the ongoing (as of June 2019) upgrade of SINFONI that is scheduled for commissioning in 2020. Figure 2 shows a schematic of the ERIS upgrade. ERIS improves upon the SINFONI instrument in several ways. It has an upgraded spectrograph, ERIS-SPIFFIER which will cover the wavelength range 1 - 2.5 μm and will offer two spectral resolutions, R = 4000, and R = 8000, both of which are higher than currently available on SINFONI. The instrument is also designed to work with the VLT Adaptive Optics Facility (AOF) which uses a deformable secondary as well as LGS. This will allow for enhanced angular resolution over SINFONI. Lastly, ERIS will also contain the ERIS-NIX imaging module. NIX will allow direct imaging with AO capability from 1 - 5 μm. It also has a coronograph which will allow for direct imaging of wide-separation exoplanets.

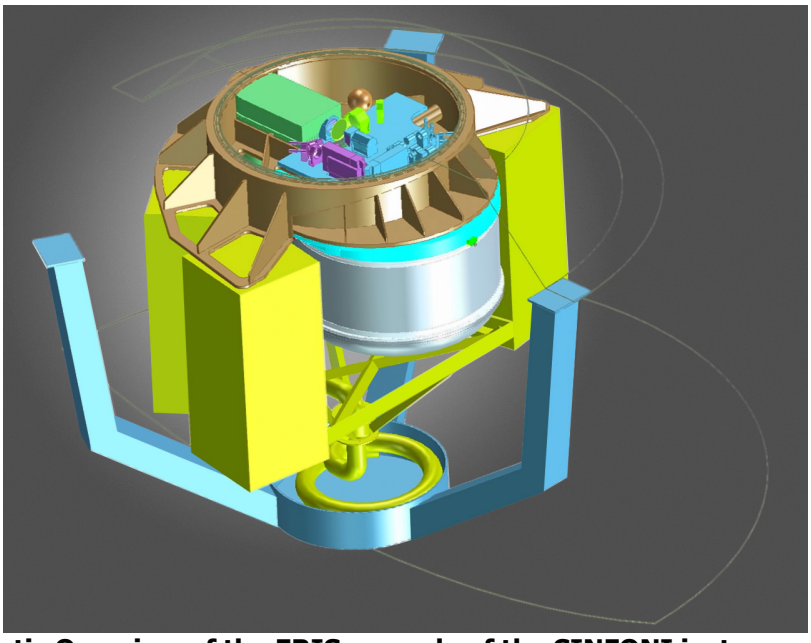

Figure 2: Schematic Overview of the ERIS upgrade of the SINFONI instrument.

5.1.2. OSIRIS on Keck

5.1.2.1. Overview of OSIRIS*

OSIRIS is an IFU spectrograph designed to work with the Keck Adaptive Optics System (see Larkin et al. 2006). OSIRIS was commissioned on the telescope in 2006. It uses an array of tiny lenses to sample a rectangular patch of the focal plane and produces spectra at up to 3000 locations simultaneously. OSIRIS also has an internal diffraction limited camera with a 20” field of view. Both the camera and spectrograph can operate at wavelengths between 1 and 2.4 μm. The center of the imaging camera’s field is

about 20" offset from the center of the spectrograph field and both can be used simultaneously with the same or different filters. The spectrograph has plate scales of 0.020", 0.035", 0.050" and 0.100" per lenslet. The spectral resolution is R = 3800 in the three finest plate scales, but is closer to R = 3000 in the 0.100" plate scale. In the broadband mode each spectrum contains a full broad band (z, J, H or K) and a total of 16 x 64 spectra are taken. In the narrowband mode, a typical spectrum contains 1/4th of a broad band and an individual exposure contains between 16 x 64 to 48 x 64 spectra depending on the exact filter selected. The imager has a single fixed plate scale of 0.020" per pixel and suffers from some vignetting in the corners of the array.

* see https://www2.keck.hawaii.edu/inst/osiris/OSIRIS_Manual_v2.3.pdf

5.1.2.2.Science with OSIRIS

Over the ongoing 13 year lifetime of OSIRIS instrument (as of this writing in June 2019) it has made notable science contributions in several fields, this includes distant galaxies, exoplanets, and observations of the Galactic centre.

OSIRIS observations of distant galaxies focussed on the AO mode. Law et al. (2009) performed a survey of thirteen z > 2 galaxies with the LGS AO which achieved sub-kpc resolution observations. They noted high internal velocity dispersions on each spaxel, suggesting that rotation may not be the dominate mode of support for distant galaxies.

Bowler et al. (2010) observed the exoplanet HR 8799b with OSIRIS. They found the planet had notable disagreement with the predictions of atmospheric models. Overall they concluded that HR 8799b has an unusually dusty photosphere, an exceptionally low luminosity for its spectral type, and hints of extreme secondary physical parameters, HR 8799 b appears to be unlike any class of field brown dwarf currently known.

Do et al. (2009) performed observations of the star cluster near the central black hole of the Milky Way. They noted that the structure of the cluster does not have a central cusp, like most star clusters, which could have interesting consequences for the formation of the Milky Way's central black hole.

5.1.3. NIFS on Gemini

5.1.3.1. Overview of NIFS*

NIFS is Gemini-North's Near-Infrared Integral Field Spectrometer built by the Australian National University's Research School of Astronomy and Astrophysics. The original NIFS was destroyed in the January 2003 bushfires that destroyed much of Mt. Stromlo Observatory. NIFS-2 (now known as NIFS) was been rebuilt by AUSPACE Ltd., a local aerospace company, with the assistance of RSAA staff. NIFS makes use of some of the NIRI designs produced by the Institute for Astronomy of the University of Hawaii.

NIFS provides 3D imaging spectroscopy with spectral resolving power of R = 5000 over a 3.0" x 3.0" image field in the Z through K-band spectral regions (0.95 to 2.40 μm). NIFS is designed to be fed by the Gemini North Adaptive Optics system, ALTAIR, hence it is possible to achieve spatially resolved spectroscopy on scales as small as 0.1" using Natural or Laser guide stars. Coronographic spectroscopy can also be performed through use of an occulting mask.

NIFS saw first light on October 19, 2005 and has been offered to the Gemini community since semester 2006B.

* See https://www.gemini.edu/sciops/instruments/nifs/

5.1.3.2. Science with NIFS

Over its 14 year lifetime of observation (as of this writing in June 2019) NIFS has made strong contributions to various fields of astrophysics. Unlike SINFONI and OSIRIS, the highest impact work from NIFS has been the observations of the central regions of nearby galaxies which host supermassive black holes.

Gebhardt et al. (2011) measured the stellar kinematics within the central 2” of M87. They determined an accurate black hole mass for M87 and showed it to be in disagreement with estimates from outside the kinematic influence of the black hole need to be reevaluated. Likewise they demonstrated the need for additional such measurements to resolve our understanding of the high mass end of the black hole dispersion vs. black hole luminosity relation.

In a serious of papers Riffel et al. (2008) and Storchi-Bergmann et al. (2009, 2010) study the central region of the Seyfert galaxy NGC 4151 at high angular resolution to understand the relative strength of black feeding (or growth) vs. the feedback they supply to their host galaxies.

NIFS has also been used to study the kinematics of distant galaxies (e.g., Swinbank et al. 2009, Livermore et al. 2015), as well as the role of outflows and AGN feedback in distant galaxies (e.g. Alexander et al. 2010).

5.1.4. KMOS on VLT

5.1.4.1. Overview of KMOS*

The K-band Multi Object Spectrograph (KMOS) is a second-generation instrument in operation on the VLT. The instrument design employs 24 configurable arms that position pickoff mirrors at user-specified locations in the Nasmyth focal plane. The sub-fields thus selected are then fed to 24 image slicer integral-field units (IFUs) that partition each sub-field into 14 identical slices, with 14 spatial pixels along each slice. Light from the IFUs is then dispersed by three cryogenic grating spectrometers which generate 14x14 spectra with ~1000 Nyquist-sampled spectral resolution elements for

each of the 24 independent sub-fields. All 24 subfields have to be used with the same grating at a time.

The patrol field of the pickoffs is 7.2' in diameter, which is the diameter of the un-vignetted field at the VLT Nasmyth focus, thus minimizing the thermal background in the K- band. Each IFU has a square field of view of 2.8" x 2.8"; anamorphic magnification in the IFU fore-optics ensures uniform spatial sampling of 0.2" x 0.2" whilst maintaining Nyquist sampling (~2 pixel) of the spectral resolution element at the detector.

The use of focal-plane pick-off arms allows considerable flexibility in selecting targets and in particular the important capacity to deal with strongly clustered or close-paired sources. In addition to observing multiple individual sources, KMOS has the capability for integral field mapping of contiguous areas in an 8-point or 16-point dither pattern. The spectral resolution of R~3000-4000 provides velocity resolution for studies of low-mass objects and is optimal for OH-avoidance in the J & H bands. A lower resolution mode is also available in the combined H+K band.

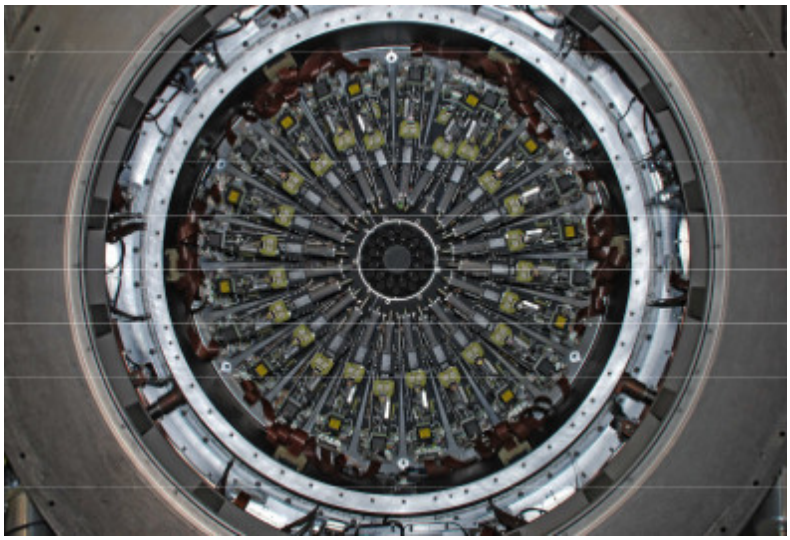

Figure 3: Image of the KMOS instrument showing the 24 pick off arms used for multi-object IFU spectroscopy.

* See https://www.eso.org/sci/facilities/paranal/instruments/kmos.html

5.1.4.2. Science with KMOS

KMOS is the newest of the NIR IFU instruments on 8m class telescopes. KMOS had first light on November 11, 2012, and has been offered for science since ESO Period 92, approximately from late 2013. In six years of science operations KMOS has focussed primarily on large surveys of distant galaxies. These surveys examine all aspects of galaxy properties from kinematics, star formation rates, metallicities and stellar

populations. While it is seeing-limited, the 24 arm capability make KMOS extremely efficient for observing large samples of distant galaxies.

The KMOS surveys include KMOS^{3D} (Wisniowski et al. 2015, Wuyts et al. 2016) a survey of > 600 galaxies at 0.7 < z < 2.7 that measured a wide range of (semi-) resolved parameters such as kinematics, star formation rates, metallicities and stellar populations. VIRIAL (Mendel et al. 2015) which is the first to focus on the properties of quiescent galaxies at z > 1 (i.e., absorption lines instead of emission lines). KROSS (Stott et al. 2016) which has measured the properties of a large sample of galaxies at z ~ 1, slightly lower than KMOS^{3D}. The KMOS Cluster Survey (KCS, Beifiori et al. 2017) which examines the properties of galaxies in galaxy clusters at z ~ 1.5 and the role of environment in galaxy formation at high-redshift. The KMOS Lens Amplified Survey (KLASS, Mason et al. 2017) examines the kinematics of high-redshift galaxies using gravitational lens amplification. Many of these surveys are similar to the science cases for GIRMOS in this document, the the difference being thet GIRMOS will do the science at higher 5-10x better spatial resolution with AO, and also with better spectral resolution.

Having been only relatively recently commissioned in 2012, and having focussed on large surveys encompassing several years of observations, the first KMOS results are only recently filtering into the astronomical community, as is illustrated by the dates on the papers cited above being within the last 2 - 3 years. As the only other multi-object NIR IFU, the results from KMOS, and its survey approach to science should and will play a key role in guiding the science goals for GIRMOS and to illustrate where and how NIR IFU survey science can be most effective.

5.2. Synergies with Other Facilities

First light for GIRMOS is currently planned for late 2027. It is clear that both the scientific landscape GIRMOS will operate in, and the landscape of observatories and instruments that it will be contemporary with from 2027 and beyond will be significantly different than the current landscape. The science cases for GIRMOS (Section 6) address the expected scientific landscape at the time GIRMOS will operate. Here we discuss the set of facilities that will operate at the time of GIRMOS and potential synergies between GIRMOS and those facilities.

5.2.1. GIRMOS and GNAO*

The Gemini North Adaptive Optics (GNAO) project will operate as the front-end AO for a Gemini AO-system that currently has GIRMOS as the only funded instrument to go behind. GNAO will deliver a queue-operated ground-layer adaptive optics (GLAO) and laster-tomographic adaptive optics (LTAO) system in the northern hemisphere. The GNAO effort will build on experience with the Gemini Multi-conjugate System (GeMS) at Gemini South, but it will employ the latest technologies for improved performance in support of the next generation of AO-assisted instruments at Gemini North. With a corrected field-of-view of about 2’ and spatial resolution similar to that of JWST, GNAO

will take advantage of Mauna Kea's outstanding conditions for AO performance and establish GN as the premier ground-based facility for wide-field AO studies.

The GNAO project was officially approved in October of 2018, which was after the CFI award for GIRMOS and only 2 months before the official kickoff of the GIRMOS project in December 2018. Originally GIRMOS was scheduled to be commissioned at Gemini-South behind the GeMS module. However, with the opportunities presented by GNAO, it was an obvious decision to move GIRMOS to the northern hemisphere to put behind GNAO. This decision was made in early 2020 and the co-development of the instruments has been in progress for several years.

* See https://www.gemini.edu/gemma/index.html

5.2.2. GIRMOS and JWST

One of the most exciting NIR IFU instruments that will operate at approximately the same time as GIRMOS is the IFU unit on the NIRSpec instrument that will fly with the James Webb Space Telescope (JWST). The NIRSpec IFU will operate at the diffraction limit of a 6.5m telescope, which is comparable in angular resolution to what will be delivered by AO with GIRMOS. The NIRSpec IFU has several advantages over GIRMOS. It has a wider range of spectral resolutions and has a wider wavelength range coverage (1 - 5 μm). Moreover, because it is located in space it does not suffer from strong sky line contamination, atmospheric absorption between the NIR filters, nor significantly from telluric absorption.

JWST will clearly have advantages over GIRMOS in spectral coverage. No lines (or in the case of galaxies, no redshifts) will be unavailable to the NIRSpec-IFU. Likewise the lack of telluric features will mean that continuum spectroscopy will be substantial easier, especially for faint targets. The NIRSpec-IFU will clearly be superior for observations of high-priority and very faint or red sources.

However, GIRMOS will dominate JWST in doing surveys of many objects. The NIRSPec IFU is just one mode of many on NIRSpec (grism, longslit, IFU, MOS), and NIRSpec is just one of four instruments on JWST. The amount of time available for NIRSpec IFU observations will be only a small fraction of the total JWST time. With four IFUs, and more flexibility in observing time, GIRMOS will be able observe much larger samples of objects than JWST.

Indeed, if the lifetimes of both instruments are long enough, it is reasonable to expect that GIRMOS surveys may identify interesting targets which then might be better followed up with ultra deep integrations on NIRSpec-IFU. How long both instruments operate concurrently remains to be seen (JWST has just launched for a 5 year mission

beginning in 2022, GIRMOS is scheduled for first light in 2027), but if they operate concurrently it can be imagined that there would be useful synergy between the two.

5.2.3. GIRMOS and Survey Projects/Telescopes

5.2.3.1. GIRMOS and CALIFA, SAMI and MANGA

Currently several extremely large optical IFU surveys are ongoing or have just been completed. These surveys, CALIFA (Sanchez et al. 2012), SAMI, (Allen et al. 2015) and MANGA (Bundy et al. 2016) have samples of 300 - 10,000 galaxies at z ~ 0 and are transforming our understanding of the distribution of stellar mass, star formation, metals and the location and strength of feedback processes in galaxies.

GIRMOS has an obvious synergy with these projects in that it will provide observations with similar angular resolution (in physical units) of galaxies at z > 0.7. The samples from optical IFU surveys will provide essential comparison samples to galaxies observed with GIRMOS. In particular, given that continuum spectroscopy will be very challenging with GIRMOS, the low-redshift samples will provide essential calibration of how well emission line (gas) kinematics relate to absorption line kinematics (stars). The latter are generally considered a better tracer of the underlying gravitational potential of a galaxy, and so will be essential for interpreting GIRMOS observations.

5.2.3.2. GIRMOS and Euclid/Nancy Grace Roman Telescope

GIRMOS has an obvious synergy with the two wide-field NIR imaging and spectroscopic missions of the 2020's, Euclid and the Nancy Grace Roman Telescope (NGRT).

Euclid is a 1.2m European Space Agency (ESA) space telescope currently being built that will survey up to 15,000 deg^2 of the sky with NIR imaging (with ~ 0.1" resolution), as well as NIR grism spectroscopy (with R = 250). Euclid will also host 3 deep fields (~ 26 AB in the NIR) covering 40 deg^2. Euclid is scheduled for a seven year mission launching in 2024, approximately the first light time of GIRMOS.

NGRT is a proposed NASA space telescope that will have a 2.4m diameter mirror and survey approximately 2500 deg^2 of the sky with NIR imaging (with ~ 0.05" resolution), as well as NIR grism spectroscopy (with R = 250). NGRT passed the preliminary design phase in May 2018 and is scheduled for launch in the mid-2020's. If it meets this launch date NGRT will also be operational simultaneously with GIRMOS.

Both of these major observatories have significant synergy with GIRMOS. They survey vast areas of sky with imaging and low spectral resolution spectroscopy. They will therefore naturally provide targets that would be followed up by GIRMOS with 10 - 20x better spectral resolution, and given the substantially larger primary mirror of Gemini, higher S/N. WFIRST and Euclid will excel at finding high-redshift NIR bright

gravitational lenses, bright galaxies and quasars at z > 6, and potentially NIR transients. All of which will benefit from followup with the capabilities of GIRMOS.

5.2.3.3.GIRMOS and PANSTARRS/Rubin/LIGO

The transient sky is becoming an increasingly exciting field. The discovery of the counterparts of gravitational wave events as well as other transient phenomenon are young fields with a large discovery space.

Gemini is one of the best-operated queue mode observatories, regularly providing rapid target-of-opportunity (RTOO) observations. Gemini is also working to enhance time domain science operations as part of the GEMMA project. GIRMOS followup of gravitational wave counterparts will be extremely exciting, as the high angular resolution of GIRMOS will allow better separation of the source and background galaxy spectral signatures.

The Rubin Telescope is scheduled for first light in 2022, and commencement of full science operations in 2023. The LSST survey with Rubin will deliver thousands of photometrically detected transient objects in the night sky each night. The NIR spectroscopic capability of GIRMOS will provide a natural follow-up tool for these transients. Gemini will in particular be well-suited to provide RTOO observations of high-priority sources.

5.2.3.4.GIRMOS and the ELTs

One of the primary motivations for building GIRMOS is for technology development for the Extremely Large Telescopes (ELTs). These observatories, The Giant Magellan Telescope (GMT, 24.5m primary mirror), The Thirty Meter Telescope (TMT, 30m primary mirror), and the European Extremely Large Telescopes (EELT, 42m primary mirror) will regularly deploy AO technology to take full scientific advantage of their large primary mirrors. Given that AO is best deployed in the NIR, provides high angular resolution, and that large telescopes are ideal for spectroscopy, instruments with multi-object NIR IFU spectroscopic capabilities are obviously of the highest priority for ELTs.

That being the case, **currently none of the ELTs have a multi-object NIR IFU scheduled as a first-light instrument**. This is for a variety of reasons, however, foremost of these was the concern of the risk of building such an unprecedented instrument for an observatory still in development. As part of risk management the TMT is building IRIS, a single object NIR AO IFU spectrograph and imager as a first light instrument. GMT is building GMTIFS, also a single object NIR AO IFU spectrograph and imager. The EELT is building HARMONI, again with similar features to GMTIFS and IRIS. Most if not all of these observatories would would like to build a MOS IR IFU as part of the second generation of instruments.

GIRMOS is currently the only funded multi-object NIR AO IFU spectrograph. The technology development for GIRMOS will clearly play an essential role for second generation instruments for the ELTs.

6. Science Cases

GIRMOS will be commissioned in 2027 and at that time will be ideally positioned as a workhorse instrument for the Gemini community. Its multiplexing capability will make it particularly efficient for large surveys, and these are likely to dominate 8m-class science in that era. By 2024 both JWST and Euclid will be operational and providing exciting new IR bright targets for spectroscopic followup. Gravity wave detectors such as LIGO in combination with imaging followup will providing well-localized gravitational wave sources. Likewise, LSST and the SKA pathfinders will be detecting exotic transient sources, and ALMA will be in an era of providing large, well-characterized surveys. GIRMOS will be the forefront AO instrument for observing large samples of the sources discovered by these state-of-the-art telescopes.

During its operations, the primary science questions GIRMOS will address are:

1) High- and low-mass star formation within the Milky Way
2) The formation process of the Milky Way super-massive black hole and its environment
3) Intermediate-mass black hole formation and chemodynamics of globular clusters
4) The nature of optical, infrared, radio, and gravity-wave transients
5) Relationship between cold gas, star formation, and dynamics in galaxies at $z > 1$
6) Ultra-high angular resolution studies of distant galaxies aided by gravitational lensing
7) Relative roles of internal processes and environment at the peak of galaxy formation
8) Galaxies, black holes and globular cluster formation processes at "Cosmic Dawn"

Here we present detailed science cases for GIRMOS and how each of these drive the requirements for the instrument. The science cases are organized into four groups: 1) Galactic Science, 2) The Nearby Universe, 3) Extragalactic Science, and 4) Star formation. Broadly speaking the Galactic and star formation science cases tend to drive the requirements on spectral coverage and spectral resolution. Extragalactic science generally involves much fainter targets and primarily drives the angular resolution and sensitivity requirements for GIRMOS.

6.1. Galactic Science

6.1.1. An AO-assisted survey probing the inner regions of Galactic Globular Clusters

Galactic globular clusters (GCs) are considered to be promising places to search for the elusive intermediate mass black holes (IMBHs, $\sim 10^2$-10^5 $M_\odot$) e.g. Portegies Zwart et al.

(2004); Giersz et al. (2015), proposed as seeds for the rapid formation of supermassive black holes in the early universe and sources of ultraluminous X-ray sources in nearby galaxies. The evidence for IMBHs in GCs is, however, still inconclusive and controversial. The shape of the velocity dispersion profile in the very central regions of GCs remains one of the best indicators of the possible presence of an IMBH, but the sphere of influence of a putative IMBH (within which the gravitational potential of the IMBH would dominate) is very small (typically ~1 arc second or smaller) and velocity dispersion measurements within this region are extremely challenging. Precise enough long-baseline proper motion measurements with HST have just started to become feasible (Anderson & van der Marel 2010; Bellini et al. 2014; Watkins et al. 2015), but are still limited and do not include enough stars inside the sphere of influence to put strong constraints on the presence of an IMBH. Another approach based on inferring the velocity dispersion from line broadening in integrated-light spectra is prone to severe "shot noise bias" due to contamination by the light of a few bright stars. Pilot studies with SINFONI (Lanzoni et al. 2013; Lapenna et al. 2015) have shown that AO-assisted near-IR Integral Field Spectroscopy is a promising alternative to measure the velocity dispersion from significant samples of individual stars (~50) in the crowded central regions of populous GCs. With the spatial resolution enabled by the Laser Tomography Adaptive Optics (LTAO) tiling mode and improved spectral resolution (compared to SINFONI), GIRMOS will open up new observations of statistically significant samples of RGB and SGB stars, allowing us to measure the velocity dispersion with sub km/s uncertainty within the sphere of influence of putative IMBHs in GCs. Should no evidence for IMBHs be detected, the same data will allow us to probe the presence of central populations of segregated stellar-mass BHs in GCs, which can also affect the kinematics in the central regions but typically inflate the velocity dispersion over a region ~10 times larger than the sphere of influence of an IMBH. Even over such a larger region of up to ~10 arc second, kinematic data in GCs is scarce, and GIRMOS has the potential to fill this gap. This is key to understand the contribution of dense clusters to the formation of BH-BH binaries (progenitors of gravitational waves) via dynamical interactions.

AO-Assisted GIRMOS Integral Field Spectroscopy probing the central regions of Galactic GCs will enable line-of-sight velocity and chemical abundance measurements of up to hundreds of individual stars in these inner (arc second scale) regions. This will yield key science regarding the formation and evolution of these systems, as well as important indications on the presence of stellar-mass (BHs) and IMBHs in their dense cores. The central velocity dispersion of a cluster is also a key measurement in determining its dynamical state and infer its properties at formation, as well as for measuring its central mass-to-light ratio to uncover populations of dark remnants. Combining kinematic information with chemical abundance measurements (of iron and other elements, such as C, N, and O) of individual stars from GIRMOS spectra will further shed light on the formation of the targeted GCs and their (multiple) stellar populations.

Additionally, measuring a cluster's central mass function and velocity dispersion profiles allows for the degree of mass segregation and energy equipartition in the cluster to be

determined (Bianchini et al. 2015; Webb & Vesperini 2016). Both of these measurements allow for the dynamical age of the cluster to be estimated, which allows for clusters to be used to probe the early Universe by placing constraints on the initial distribution of GC properties and by extension their formation environment. Furthermore, knowing how energy equipartition varies with clustercentric distance allows for post core-collapse clusters to be identified kinematically, which is particularly useful as identifying core-collapse clusters photometrically is both difficult and ambiguous (Bianchini et al. 2018).

Finally, GIRMOS is ideally suited for GCs within the Galactic Bulge. These clusters, having evolved in the stronger tidal field of the inner galaxy (compared to their halo counterparts), are generally expected to have lost a significant amount of stars to the Galaxy since formation and be dynamically old. However, very limited internal kinematic information is currently available for bulge GCs, even though they constitute a significant fraction of the Milky Way GC system. The high spatial resolution and infrared capabilities of GIRMOS are well suited for these observations, where dust and crowding mitigation is critical. Very few of these clusters are included in recent kinematic studies or compilations of proper motions or line-of-sight velocities of individual stars (e.g. Watkins et al. 2015; Kimmig et al. 2015; Baumgardt & Hilker 2018; Kamann et al. 2018). Chemical abundance studies of bulge GCs could also reveal systems with a complex formation history like Terzan 5, a bulge GC reported (based on near-IR photometry) to host two stellar populations with different iron contents and ages, and which could be the surviving merger remnant of primordial building blocks of the bulge (Ferraro et al. 2009).

6.1.1.1. Observational Requirements

Observations of the dense cores of GCs will require to use GIRMOS in a 'tiled' IFU mode to take full advantage of the unprecedented combination of spatial and spectral resolution over a large FOV offered by tiling (R~8000, 50 mas/pixel; over a 4x4" FOV; see Figure 4). This mode will use LTAO.

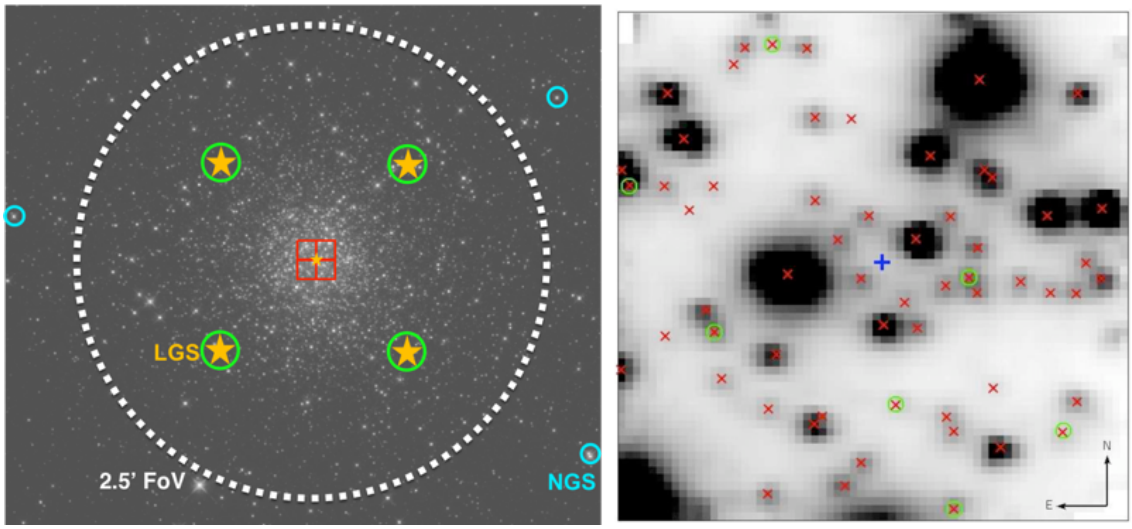

Figure 4: Left: The `tiled' IFU mode for GIRMOS superimposed on the center of the Globular Cluster Terzan 5 (also shown is the GeMS LGS asterism). This mode offers 50 mas/spaxel spatial resolution and probes a 4.2x4.2" FOV; nearly identical to the predicted 3.5"

To specify the observational requirements in terms of spectral resolution and AO performance and also gauge how GIRMOS will perform compared to contemporary methods, we extrapolate the observations of Lanzoni et al (2013). These authors used SINFONI+AO to observe the central 3x3" of the Bulge GC NGC 6388. The observations were done at K-band with R~4000 and in a few hours of observing time they measured the line-of-sight velocities (with 2 km/s precision) for 60 individual stars to put an upper limit on the mass of a putative IMBH. Given the same observation with GIRMOS, an increased spectral resolution (~8000) would lead to an improvement in the velocity precision for individual stars to sub km/s (see Hatzes 1992) and an AO improvement (from 30-60% Strehl) would lead to a doubling of the signal to noise per star. The latter point allows for an increased sample size of ~50% (roughly calculated due to the improvement in both spatial resolution and signal to noise). Both requirements allow, for example, to measure changes of 30% or less in the velocity dispersion within the central arcseconds at the 3σ level. The increase in spectral resolution and SNR would also allow us to derive metallicities for all of the stars in the kinematic sample (see Do et al. 2015 for the type of analysis that would be used). Additionally, we aim to take advantage of the increased spectral resolution of GIRMOS in order to constrain individual chemical abundances for each of these stars; the use of convolutional neural networks will be explored to make these constraints (following Fabbro et al. 2018).

6.1.2. Stellar Chemodynamics of the Nuclear Star Cluster Around the SMBH of the Milky Way

The metallicity distribution function (MDF) of the Galactic Bulge shows a metal-rich population and long tail of stars with lower metallicities. Before chemical information was available, the cluster appeared to be rotating in the plane of the Galaxy and did not display major irregularities. Recent metallicity measurements show the rotation signature

is much weaker in the low metallicity population, which can tell how the cluster might form, and most of the metal-poor stars are all moving with roughly the same velocity (Do et al., in prep), potentially indicating a cluster in-fall into the Galactic Center. A larger sample of chemodynamical measurements will help shed light on this picture and is currently unfeasible for single AO-fed IFU observations with current facilities given their relatively small FOVs when using high spatial resolution modes. Additionally, individually tiled IFU observations cover a limited space about the Galactic Centre; to get deeper longer integrations are required, which is much more feasible with a multi-IFU instrument like GIRMOS. In addition, a deeper, larger sample size at the Galactic Center will allow us to study star formation in an extreme environment; this is achieved by monitoring the collection of stars over time by looking at the binary fraction. Binarity at the Galactic Center affects the dynamical evolution of the nuclear star cluster, and if the Galactic Center observation campaign is observed over several epochs then this fraction may be measurable through radial velocity variation in spectral features.

6.1.2.1. Observational Requirements

Based on previous observations of the nuclear star cluster with NIFS + Altair with a 3x3" FOV (Stostad et al 2015; Do et al. 2015); we predict a sample size of ~ 200 stars in a 4.5 hour integration at K band. Such a large sample size would be critical in reconstructing the chemodynamical model of the nuclear star cluster. However, to encapsulate the entire nuclear cluster the FOV of these observations would need to be extended to ~10x10". We will employ the 'tiled mode' of GIRMOS (which offers a 4.2x4.2" FOV (50 mas/pixel) and up to an 8.4x8.4" FOV for a lower spatial resolution 100 mas/pixel - the same sampling as Do et al. 2015). The improved adaptive optics correction from LTAO requires the higher sampling mode (50 mas/pixel) of GIRMOS; this would increase the sample size and the SNR for each star in such an observation. Encapsulating the entire cluster would require 4 'tilings' of the 50 mas/pixel mode. We aim to measure the chemodynamics of at minimum 200 stars within the cluster. A SNR of at minimum 30 per spectral pixel is required for each star to compute metallicities and potentially individual abundances.

6.2. The Nearby Universe

6.2.1. Nearby Starburst Galaxies

The early assembly of large galaxies was almost certainly a violent process, involving the successive merging of smaller systems. The resulting interactions would have stirred the interstellar mediums (ISMs) of the merging systems, causing large-scale motions in the ISM and collisions between giant molecular clouds, thereby stoking elevated levels of star-forming activity. The formation of globular clusters and the growth of bulges and central nuclei are just three likely consequences of such events. Starburst galaxies are thus in a stage during which key components of their future morphological properties are being defined.

Starburst activity is remarkably common among nearby galaxies, suggesting this activity continues to be an important part of galaxy evolution even at the present day. Nearby starburst galaxies provide an opportunity to glimpse conditions that may have been prevalent during the early stages of galaxy assembly. Curiously, while some nearby starburst systems are triggered by interactions (e.g. M82), some galaxies have elevated levels of star-forming activity without an obvious trigger (e.g. NGC 253, M83).

The stellar content in the central kpc of nearby starburst galaxies is of particular importance for understanding more distant systems. The dissipation of energy in the ISM and the onset of inflows caused by interactions act to make the star formation rate (SFR) in a starburst galaxy to be highest in its central regions, where the gravitational well is deepest. The inflow of material from larger radii, coupled with a higher threshold for retaining material that may otherwise be blown out at larger radii, act to keep star-forming activity going in the central regions of a galaxy after the SFR has died down at larger radii. The center of a galaxy is thus an environment where large-scale star formation begins early-on in a starburst, and is also the last place for it to die out. The central regions of starburst galaxies thus contain a fossil record that spans almost the entire duration of starburst activity.

Observations of the central regions of nearby starburst galaxies reveal large numbers of clusters and star-forming complexes. Such stellar concentrations are of interest as their ages can be determined free of contamination from any background population that formed prior to the onset of starburst activity. This in turn allows the age of the starburst to be determined, and the chronology of star formation in this environment to be examined.

There are a number of questions that can be addressed through a spectroscopic study of the central regions of nearby starburst galaxies. For example, has the SFR been continuous? Or have there been periods of decreased star-forming activity due to feedback? Is there a young cluster associated with the nucleus of the galaxy and - if so - at what rate does the stellar mass of the nuclear cluster grow with time? Are the HII nuclei that are common in nearby galaxies relics of starburst activity? Is there evidence for a radial age gradient within the central kpc? How does the radiation field of a large cluster affect the surrounding environment? (e.g. is there evidence for propagating star formation?) What is the depletion timescale for star-forming material? Is the IMF in starburst regions similar to that in galaxies with more sedate star-forming activity? How does star formation progress in the nuclear regions of galaxies where super-massive black holes (SMBHs) might be present, and how does this compare with galaxies that lack SMBHs?
A large survey of the central regions of nearby ($d < 20$ Mpc) starburst galaxies will provide a transformational opportunity to probe the mechanics of starburst activity. The requirements and details of such a survey are described in the next section.

6.2.1.1. Observational Requirements

Wavelength Coverage: Given the dusty nature of star-forming regions then observations at wavelengths longward of 1μm are essential to overcome the expected high levels of extinction. The near-infrared also contains astrophysically important diagnostics of stellar content - absorption lines in the 1 - 2.4μm wavelength region trace populations with ages > 10 Myr while emission lines of atomic and molecular hydrogen and atomic helium at these wavelengths probe younger populations (e.g. Figure 5).

Angular Resolution: The central regions of galaxies are crowded environments, and the pressure exerted by the hot ISM in starbursts can produce compact clusters. Angular resolutions that are better than those delivered by free-seeing instruments are required to cleanly identify and isolate individual star clusters, and sub-structure within them. The investigation of sub-structure is important as many of the star-forming regions are not simple stellar populations, but are star-forming complexes containing stars spanning a range of ages (e.g. Figure 6).

To set requirements for angular resolution we consider galaxies at the extremes of the distance range that would be sampled with this program. The nearest starburst galaxies are at distances of ~3 Mpc. The half mass radius of compact clusters is typically a few parsecs, and so angular resolutions in the range 0.1 – 0.2 arcsec are required to resolve these structures in the nearest starbursts. As for galaxies in the Virgo cluster, it will not be possible to resolve the cores of compact clusters. However, sub-structuring within central star-forming complexes occurs on spatial scales on the order of 10 parsecs (e.g. Figure 6), and at a distance of 10 - 20 Mpc then sub-structuring can be resolved with angular resolutions in the range 0.1 – 0.2 arcsec.

Spectral Resolution: The emission and absorption features that would be targeted are broad and very prominent, and so very high spectral resolutions are not necessary; for example, the ISM in starburst environments is kinematically hot, with velocities of 100 km/sec. Spectral resolutions in the range 1000 – 3000 would be suitable for this program. The Need for IFUs: The central regions of a starburst galaxy are complicated environments, with overlapping structures. Single slit spectroscopy cannot adequately probe such an environment. An IFU capability is essential to allow sub-structures to be identified and mapped in central star-forming complexes. It is also beneficial to identify contamination from non-cluster members.

Multiplexing: The ability to deploy multiple IFUs results in a significant multiplex advantage in the nearest star burst systems, as there are numerous clusters and star-forming complexes in their central regions. The ability to position the IFUs to form a super-IFU is also of interest to allow a survey of the circum-nuclear environment in these systems.

Northern or Southern hemisphere? There is not a hemispheric preference for this program, as the distribution of targets on the sky is more-or-less uniform. Nearby starburst galaxies are present in the Sculptor and Centaurus groups in the Southern hemisphere, and in the M81 and Maffei 1 groups in the Northern hemisphere. A prime target is the Virgo cluster, and it is observable from both Chile and Hawaii.

Time needed to conduct this program: Based on the number of starburst galaxies in the closest galaxy groups (Sculptor, Centaurus, M81, and Maffei 1) then simple scaling arguments suggest that there are on the order of 50 starburst galaxies within 10 Mpc. The Virgo cluster contains a similar number of active systems. Assuming one hour exposure times (based on the observations of the nucleus of NGC 253 discussed by Davidge 2016, ApJ, 818, 142) and two exposures per galaxy, then a volume-limited survey of starbursts and an examination of Virgo could be conducted in ~200 hours total exposure time with GIRMOS.

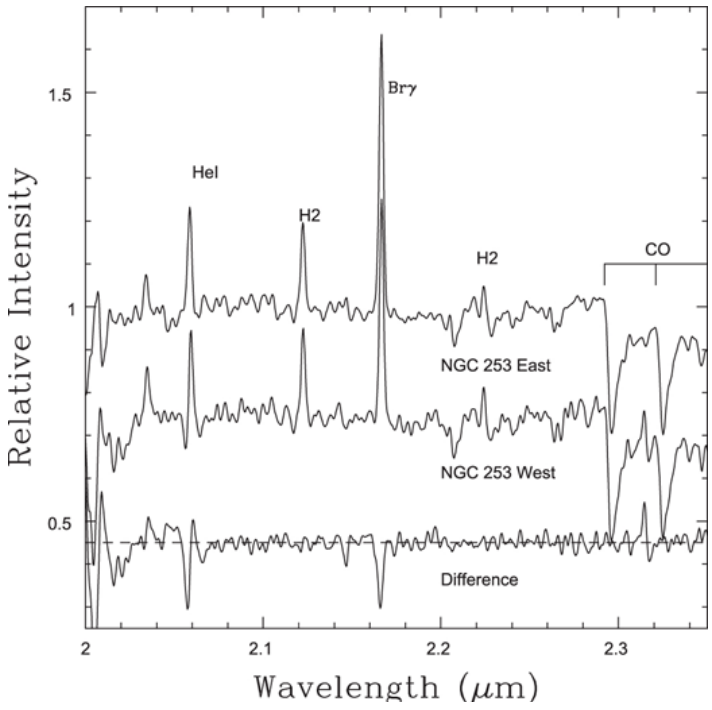

Figure 5: The K-band spectra of two regions near the center of the nearby (D ~ 3 Mpc) starburst galaxy NGC 253. The spectra were extracted from GNIRS IFU observations on Gemini South. Various emission and absorption features that are probes of stellar content are indicated. The Br˙Y and HeI lines probe hot stars, with the HeI line originating in Wolf-Rayet stars. The H2 lines probe the ISM, while the CO bands originate in evolved red stars, with the largest contribution from red supergiants and asymptotic giant branch stars. Differences between the two spectra are evident, indicating that the stellar content near the center of NGC 253 is not uniformly mixed. From Davidge (2016, ApJ, 818, 142).

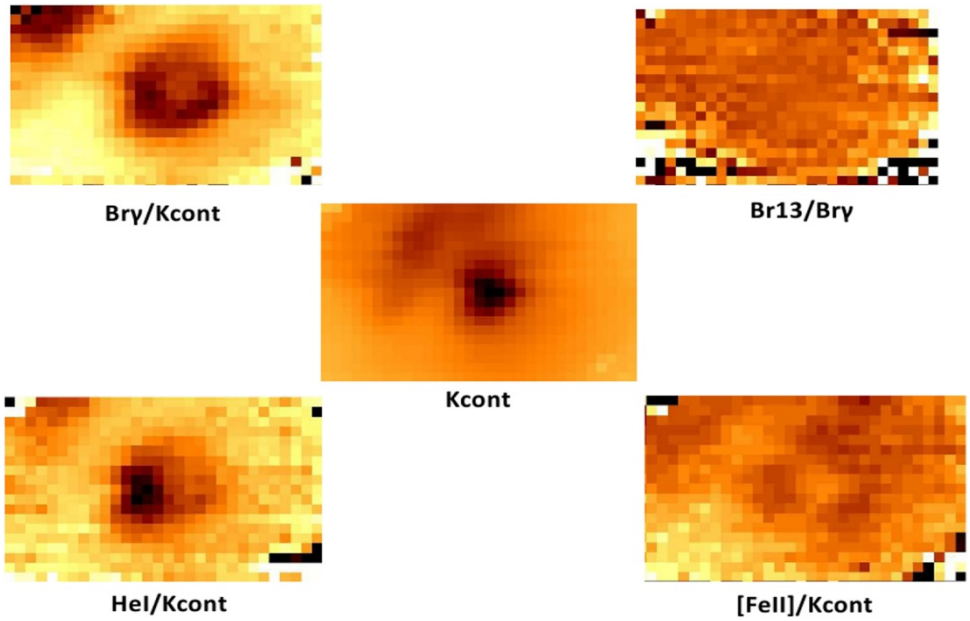

Figure 6: Maps of various emission lines constructed from GNIRS IFU spectra of the central regions of NGC 253. Each map covers roughly 5 x 3 square arcsec. The central structure in the Kcont image is the galaxy nucleus, and this area is an area of recent star formation. The differences in the distributions of Br'Y and HeI indicate that recent star formation has had a complex spatial distribution. The youngest, hottest stars (Wolf-Rayet stars with ages < a few Myr) produce the HeI line, and it is evident that these objects are concentrated to the lower left of the nucleus in these figures. In contrast, the stars that produce Br'Y emission (blue stars with ages < 10 Myr) occur over a wider area. The [FeII] line can originate in SNe and HII regions. That this line is found around the nucleus favors a SNe orign. If this is the case then the nuclear regions of NGC 253 may be in the process of being purged of star-forming material. With GIRMOS it will be possible to explore the center of NGC 253 with much higher angular resolutions and also probe star-forming complexes that surround this field. From Davidge (2016).

6.3. Extragalactic Science

6.3.1. An AO-Assisted Survey of 0.7 < z < 2.7 Field Galaxies: Insight into Dynamical Processes That Drive Galaxy Mass Assembly

Stellar mass growth of galaxies during their star-formation phase and the transformation of star-forming systems into quiescent population are two key processes in galaxy evolution. The growth of star-forming galaxies near the peak epoch of star formation is regulated through the interplay between smooth accretion and/or mergers and feedback from star formation and active galactic nuclei (e.g, Clauwens et al. 2018, Snyder et al. 2017, Rodriguez-Gomez et al. 2017, Sparre 2015, Dekel & Mandelker 2014). Merger and feedback processes play an important role in quenching of star formation at this redshift (e.g., Pontzen et al. 2017). Studies of spatially resolved kinematics and emission line properties of galaxies at "cosmic noon" covering a wide range in stellar mass and star formation rates can probe the effects and constrain relative contribution of these processes to the transformations in galaxy stellar mass, metallicity, stellar population age,

morphology, and dynamical state from the peak of their star formation activity to quiescent stage.

Current AO-assisted IFS surveys provide exquisite samples of up to ~30 galaxies with emission line properties uniformly sampled on 1-2 kpc scale, revealing their spatially resolved dynamical properties and radial variations in metallicity (e.g., SINS/zC-SINF; Förster Schreiber et al. 2018a and the references therein). However, larger statistical samples are required to further probe dynamical processes that drive galaxy evolution by 1) quantifying the fraction and structure of mergers and non-mergers, 2) mapping the demographics of turbulent disks and tracing their origin, 3) probing the strength of galactic outflows on a range of spatial scales, 4) investigating the connection between merger events and the nature of compact dispersion-dominated objects, and 5) tracing the growth of bulges.

Multiplex near-IR IFS systems enable surveys with representative samples that can trace the transformation of galaxies from star-forming to quiescent phase (KMOS^{3D}, Wisnioski et al. 2015). Although targeting an unprecedented number of several hundred $0.7<z<2.7$ galaxies, this IFU survey is limited by its natural-seeing resolution. With angular resolution of ~0.5", the survey provides Hα maps that reveal galaxy dynamical properties sampled on a scale of 4-5 kpc for $z>1$ targets (Wuyts et al. 2016, Lang et al 2017, Belli et al. 2017, Übler et al. 2017, Wisnioski et al. 2018, Förster Schreiber et al. 2018b).

A combination of high-resolution AO-assisted IFS and multiplexing capabilities of GIRMOS provides an opportunity to observe the effects of accretion, mergers, and feedback processes on ~1 kpc scale for large samples of galaxies at $z>1$. Based on the evolution of galaxy number density over the $1<z<3$ redshift range (e.g., Muzzin et al. 2013), the area of the IFU patrol field will include several massive star-forming galaxies in each $\Delta z=0.2$ redshift bin within this range. Four deployable IFU heads performing simultaneous observations will enable a build-up of statistical galaxy samples with spatially and spectrally resolved emission line properties.

Fluxes and profile shapes for a number of rest-frame emission lines – H_β, [OIII], [NII], H_α, [SII] – measured with ~ 1kpc spatial resolution will provide testbeds for quantifying the importance mergers for galaxy mass assembly (see Figure 7). Mergers with different mass ratios have different effects on galaxy dynamical properties. The imprints of major mergers are multiple dynamical galaxy components, disrupted rotational velocity fields, and significant off-center peaks in velocity dispersion fields. In contrast, minor mergers (accretions) will cause a minor disruption to the velocity field of the more massive galaxy. In addition to direct measurements of fractions of different types of mergers over a broad redshift range, the maps of emission line ratios, providing radial distribution of metallicity gradients, will probe the contribution of galaxy interactions to their chemical evolution.

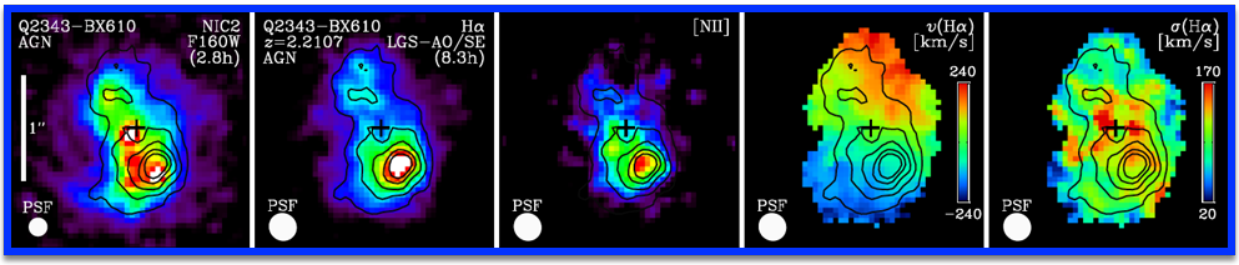

Figure 7: Adapted from Forster Schreiber et al. (2018). From left-to-right, maps of a galaxy in F160W, H-alpha, [NII], H-alpha velocity offset, H-alpha dispersion. With it's multiplexing capability, GIRMOS will provide similar maps of hundreds of galaxies at 0.7 < z < 2.7.

The emission line maps will provide spatially resolved maps of AGN and star formation activity diagnostics (i.e., spatially resolved BPT diagrams). Additional processes proposed to drive galaxy transformation from star-forming to quiescent stage can also be probed through line profile fitting of spatially resolved emission lines in the rest-frame visible regime.

Galaxies with prominent AGN exhibit massive fast outflows detected on kpc-scale in ionized gas as an additional component of emission line (e.g., [OIII]) with large velocity offset (~600 km/s) and large velocity dispersion (~1000 km/s, e.g., Karouzos et al. 2016a,b). The nature of this feedback mechanism remains an open question. Although AGN driven outflows carry significant amount of gas, a fraction of this material may remain in galaxy halo and fall back to replenish gas reservoir for star formation at later times (Arribas et al. 2014). In this scenario fast outflows would not produce a global shut down of star formation. In addition, existing (small number of) IFU observations suggest that a fast outflow depletes gas reservoir only along its path, leaving the star formation rates in other regions intact (Carniani et al. 2016). Finally, outflows can also induce star formation in galaxy disk (Silk 2013) and/or outflowing material (Ishibashi & Fabian 2012). GIRMOS will provide statistical samples of active galaxies with observations of outflows on kpc-scale that are critically important for testing the "preventive" and "positive" feedback scenarios.

6.3.1.1. Understanding environment with GIRMOS simultaneous imaging

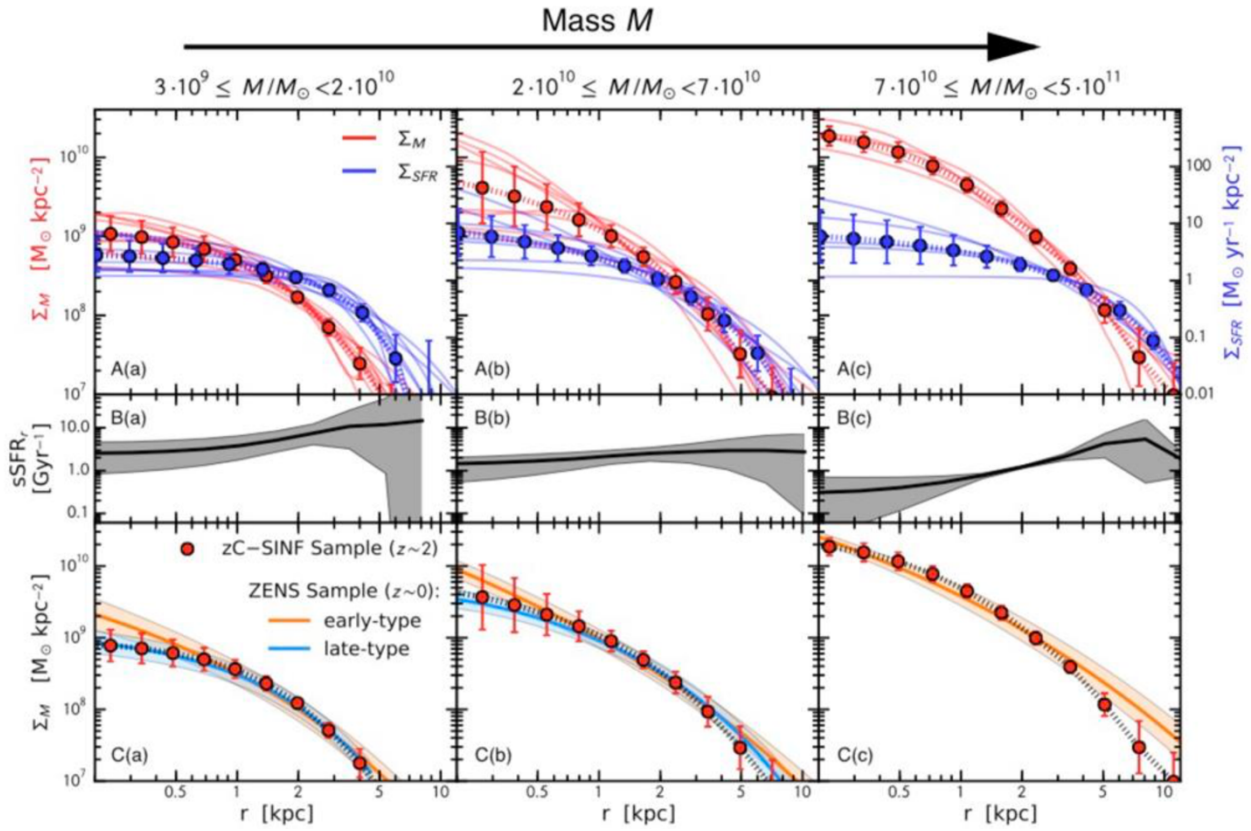

Figure 8: Surface density of star formation (blue) and stellar mass (red) vs. radius for nearby galaxies (top panels), and z ~ 2 galaxies (bottom panels). Each column represents galaxies of different masses. These observations show that z ~ 2 galaxies have star formation at similar location as their stellar mass, but z ~ 0 galaxies have little star-formation in their core, primarily in their outskirts showing they grow inside-out.

Correlating the location of star formation, determined with GIRMOS spectroscopy, with the existing stellar mass will provide critical clues as to where and how galaxies built up their structure over time. Figure shows early results on where the stars in galaxies are, versus where the star formation is. This figure is from Tacchella et al. (2015, Science, 348, 314), where they mapped star formation in 22 galaxies using Hα emission using the LGS AO mode of VLT/SINFONI and correlated this with the stellar mass determined from Hubble Space Telescope broadband imaging of the same galaxies. Their results suggest that galaxies grow in an "inside out manner", with star formation occurring in the central regions at early times, and later migrating to the outer regions. While enticing first results, we clearly need representative samples in order to understanding how this process works as a function of galaxy mass and redshift.

GIRMOS spectroscopy will provide the necessary resolved H-alpha spectroscopy to measure resolved star formation (Section 6.3.1), but high-resolution broad band imaging is necessary to determine the location of stars. Currently such work is slated to be done with HST/JWST imaging; however, requiring HST/JWST imaging for all galaxies is extremely limiting, in that it requires only selecting targets from fields with existing HST

observations, or requires obtaining HST/JWST imaging for galaxies observed with GIRMOS.

The ability of GIRMOS to provide simultaneous broadband imaging and spectroscopy of extragalactic fields will make the combined system the most powerful survey instrument of its kind by far. While JWST is faster for deep imaging, GIRMOS can provide this imaging at no extra cost while it is obtaining spectroscopy. Of course, the imaging/spectroscopy of a field cannot be truly simultaneous (the probe arms will obscure the spectroscopic targets during observations), most spectroscopic programs plan to observe the same field multiple times, putting the probe arms on different targets at each visit (the typical source density of target galaxies per GIRMOS field is 20 – 40, but GIRMOS has only 4 IFUs). When the probe arms are placed on different targets, the previous targets can be imaged with GIRMOS. Typical spectroscopic integration times will be 5 – 15 hours, and therefore the simultaneous imaging will be exquisitely deep, and extremely powerful for the key science goal of studying the evolution of galaxy structure. Moreover, with the imager as a subsystem of GIRMOS, these measurements will be obtained *at no additional observing cost* making GIRMOS the ultimate resolved galaxy evolution survey instrument.

6.3.1.2.Observational Requirements: spectroscopy

Spatially resolved maps of the kinematic properties of gas in star-forming and/or active galaxies at z~1.5-2 must be sampled at the physical scale of ~1 kpc (i.e, within the half-light radius). This physical scale corresponds to an angular scale of 0.1”-0.2”, which is achievable with AO corrected observations. Velocity dispersion and metallicity/BPT diagnostics line flux measurements require spectral resolution of R~3000.

The most logical set of targets for a large survey of galaxies would be selected from the parent 3D-HST galaxy sample with WFC3 G141 low-resolution grism spectra, redshift estimates, and measured integrated emission line fluxes. In emission line galaxies the typical line fluxes (for Hα, Hβ, [OII], [OIII] lines) are within the 10^{17}-10^{15} erg/s/cm^2 interval (Momcheva et al. 2016). To ensure adequate S/N for spatially resolved emission line detection and modeling, we require a S/N = 5 per spatial resolution element, per spectral resolution element at one effective radius for a typical “main-sequence” disk galaxy at z = 1.5 with a SFR = 20 $M_{\odot}yr^{-1}$. Based on AO-assisted NIFS integration time estimates, these flux levels and S/N require and integration time (on source) of 5-30 h for observations in H-band.
For galaxies at 0.7<z<2.7 with a range of integrated emission line flux measurements the average observing time per target (including ~30% overhead) is 20h. With four targets being observed simultaneously, a representative sample of 80 galaxies can be assembled in 400 hours.

6.3.1.3. Observational Requirements: simultaneous imaging

Ability to obtain deep photometry simultaneously with spectroscopy is critical

Sensitivity: Typical targets are described in Section 6.3.1. Those at the faint end correspond to H = 25. At z ∼2.5, this corresponds to Log(M*/Msun) ∼ 9.5, the lowest mass galaxies that are planned to be targeted. This should be observable at SNR > 5, and should be obtained without adding additional time to the spectroscopic observations i.e., in 5 hours.
Requires broad band filters (J, H, Ks)

6.3.2. Resolving Disk Growth at 2 Gyrs after the Big Bang

High-resolution deep optical images taken with the Hubble Space Telescope in the 1990s revealed a substantial fraction of irregular star-forming galaxies at z > 1 (Glazebrook et al. 1995; Abraham et al. 1996), suggestive of major mergers and violent star-bursts dominating at early times. However, key results over the last 15 years, particularly with the advent of 3D spectroscopy and sensitive near-infrared (NIR) detectors, have revealed that a majority of these irregular galaxies at z ∼ 1–2 are actually "normal" disk-like systems hosting vigorous star-formation (Wuyts et al. 2011, Wisnioski et al. 2015, Stott et al. 2016). While hierarchical merging is still an important part of the galaxy evolution story, a new narrative has emerged such that galaxies preferentially live in a state of equilibrium – with gas in galaxies settling into disks on short time scales regardless of their merger/accretion history (Bouche et al. 2010). At the same time, complementary observations have traced the evolution of properties governing this equilibrium state from z ∼ 0–3, e.g. increased molecular gas fractions (Saintonge et al. 2013) and velocity dispersions (Wisnioski et al. 2015), and decreased dark matter fractions (Ubler et al. 2017).

First indications at z ∼> 3 suggest that there is a rapid decline in disk fractions to ∼< 40% and rising velocity dispersions (Gnerucci et al. 2011, Turner et al. 2017, see Figure 9). Is this a consequence of observational limits imposed by surface brightness dimming and size evolution (Allen et al. 2017) or is there an important transition affecting the settling of gas in galaxies at z = 3 – 4 and beyond? Tantalizingly the first resolved observations of z ∼ 6 – 7 galaxies with ALMA reveal marginally stable disks similar to z ∼ 2 observations (Smit et al. 2018) seemingly in conflict with the declining fractions mapped from z = 0 – 3.

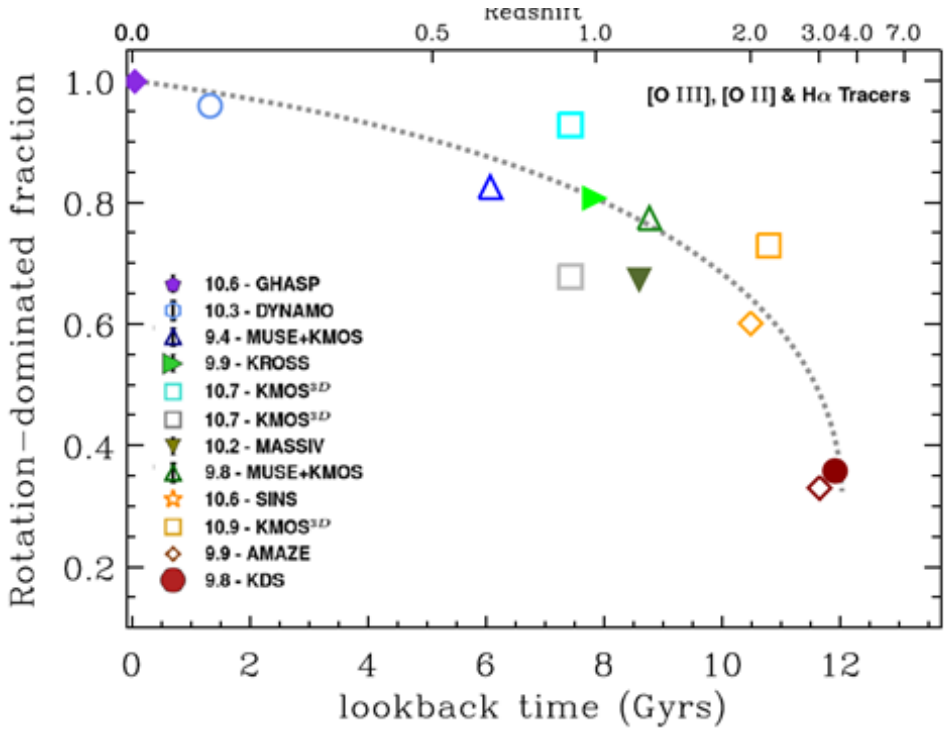

Figure 9: Evolution of rotation-dominated galaxies ($V/\sigma > 1$) as a function of loopback time. A steep rise is seen between 2.5 < z < 3.5. At present only 14 galaxies a z > 3 exist with AO-assisted observations.

The number and quality of z ~ 3 resolved data are limited. Resolved spectral observations are difficult and time consuming due to both size evolution (galaxies are 1.5× smaller than at z ~ 2 at fixed mass; Allen et al. 2017) and increased surface brightness dimming. KMOS and MUSE are unsuitable due to their relatively course 0.2" sampling in seeing-limited conditions, with a 0.5" PSF corresponding to 2× typical half-light sizes of massive galaxies. Consequently, there exist only ~ 14 non-lensed galaxies with AO-assisted observations at z > 3 with typical exposure times of just 4-5 hours (Law et al. 2007, Lemoine-Busserolle et al. 2010, Gnerruchi et al. 2011). For the brightest galaxies, these exposure times may be sufficient. However, observations over the last 5 years have highlighted the absolute necessity of deep IFS observations to correctly classify galaxy kinematics - probing out to 2-3x the effective radius of the galaxies (Forster Schreiber et al. 2018, Fig 9). Thus, the highest quality data and most impactful results arise from 8+ hour observations (see SINS & KMOS surveys all of which have relied on guaranteed time observations).

Even a modest multiplexing capability with GIRMOS will give a large advantage over existing AO facilities making a statistical sample of ~ 50 galaxies feasible. GIRMOS observations of z~3 galaxies would reveal their OIII velocity fields, line-of-sight turbulence, and the presence of large scale winds. With a well selected sample of 50 massive galaxies, a more robust disk fraction can be calculated to determine if the rise of disk galaxies at z~2 is as rapid as currently indicated or if disks commonly formed in

the first two Gyrs after the Big Bang. A project of this scope presents clear synergies with dust and molecular gas studies already being led by ALMA to characterize mass budgets and turbulence in similar samples.

6.3.2.1. Observational Requirements

To create a unique advantage in order to push into the $z \sim 3$ regime, GIRMOS will need multiplexing, adaptive optics, and large IFUs.

Spaxel sampling of 0.1" and a 0.17-0.2" PSF FWHM, are needed resolve $z \sim 3$ SFGs to $\sim 2-3 \times r_e$ allowing resolved [O III] velocity and velocity dispersion fields. This sampling corresponds to ~1 kpc resolution. While even finer spatial sampling would be preferred it may be prohibitively time expensive and better suited for follow-up of targets observed with 0.1" resolution that show interesting structure.

Additionally large 4" IFU size with 0.1" sampling are ideal because they allow for on-source dithering saving a factor of $\sim 1.3-2\times$ loss typically incurred with nodding to the sky throughout the night to remove the highly variable NIR sky. With typical sizes of ~1-2 kpc, a smaller IFU would not be sufficient to nod the galaxies within the IFUs.

An $R > 3000$ mode will allow the decomposition of galactic scale winds from broad outflowing emission components typical in massive star-forming galaxies (Ho et al. 2016; Forster Schreiber et al. 2018b). This sample would allow for the first time a statistical look at dynamics, morphology, and outflows just 2 Gyrs after the Big Bang, able to answer questions about the onset time of the equilibrium state of star-forming galaxies and the structures they evolve into over the subsequent ~ 12 Gyrs. Observations (Wisnioski et al. 2015, Turner et al. 2017) indicate that a higher spectral resolution for high mass galaxies at this epoch is likely not needed as current observations indicate line of sight velocity dispersions >50 km/s.

Assuming these requirements are met, this project will require ~130 hours to obtain a K-band selected sample of 50 massive ($> 10^{10.2}$ Msun) star-forming galaxies – an increase over current AO numbers by a factor of 4.

6.3.3. Dusty Star Forming Galaxies (DSFGs) at z > 2

With >100 times the star formation rate (SFR) of our Milky Way (or 850μm fluxes of S850μm > 3 mJy) DSFGs are most prevalent ~10 Gyr ago when the cosmic star-forming activity peaks ($z \sim 2.5$; e.g., Chapman et al. 2003, 2005; Simpson et al. 2014; Chen et al. 2015). Their extreme star formation rates $> 300 M_\odot\ yr^{-1}$ allow them to consume all their cold gas reservoir within 100 Myr (e.g., Bothwell et al. 2013), and potentially double their stellar masses within their short but blazing lifetime (e.g., Magnelli et al. 2012). Their ability to quickly form up to $10^{11}\ M_\odot$ of stars makes them candidates of progenitors

of z=1–2 compact quiescent galaxies (Toft et al. 2014) and local massive ellipticals (e.g., Simpson et al. 2014). Moreover, due to their high SFRs, DSFGs contribute over one third of the total cosmic star formation rate density over z=1–4 (e.g., Swinbank et al. 2014) representing an essential population for models of galaxy formation and evolution.

However, theoretical models have come to a diverse set of conclusions regarding the physical processes that trigger DSFG star formation: low-mass merging starbursts, with unusually low mass-to-light ratios (Baugh et al. 2005; Swinbank et al. 2008); isolated (or not-strongly interacting), gas-rich disk galaxies with secular bursts (e.g., Davé et al. 2010; Cowley et al. 2015); and a hybrid of merger-induced starbursts and secularly evolving disks (e.g., Hayward et al. 2013). One way to distinguish between mergers and disks is to search for irregular morphologies, tidal features, or spiral arms in the stellar emissions in deep rest-frame optical/NIR imaging. However, recent studies of DSFGs from the Hubble Space Telescope have shown mixed results. While the rest-frame optical light profile of DSFGs resemblances local disk galaxies (e.g., Targett et al. 2013), visual inspection reveals that over 80% of them have irregular morphologies or are merging systems (Figure 10; Chen et al. 2015). Moreover, patchy dust obscuration makes separating mergers from disks even more challenging (e.g., Mortlock et al. 2013).

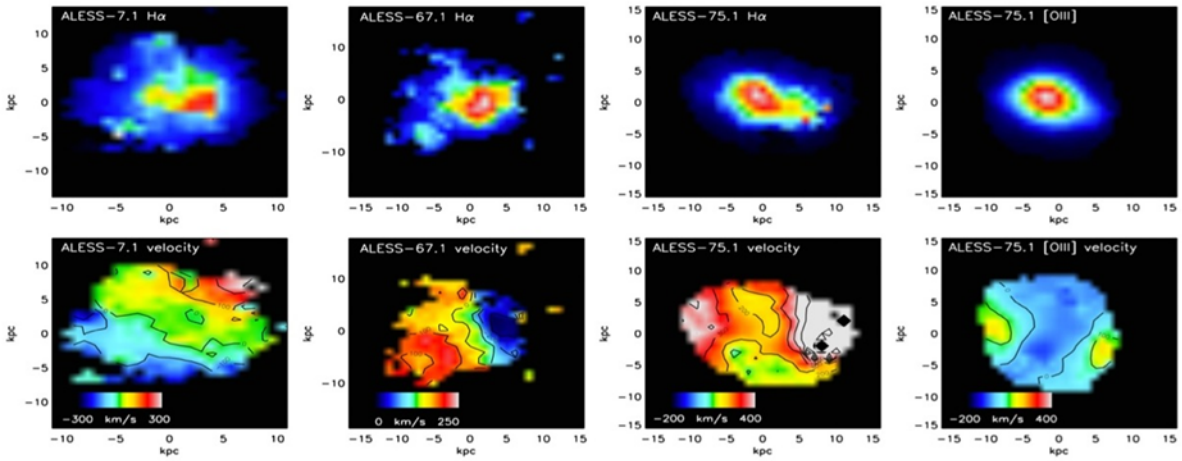

Figure 10: Hα maps and velocity distributions for three ALMA-identified DSFGs observed with SINFONI-AO. ALESS7.1 and 67.1 (left two DSFGs) demonstrate disk-like velocity structure whereas ALESS75.1 (right panels) appears to be more disturbed.

To make progress in the study of DSFG triggering mechanisms, we need to observe the distributions and kinematics of the gas and star formation to search for evidence of highly disturbed interactions (mergers) or ordered rotation (disks).

Large samples of DSFGs (~5000) now exist at z > 2 thanks to surveys like the 5 deg^2 SCUBA-2 Cosmology Legacy Survey (S2CLS) (Geach et al. 2013), which have been followed up with high spatial resolution sub-mm imaging using the ALMA and SMA interferometers.

Many of the brightest sources break up into groups of star bursting galaxies, each still lying well above the main sequence of star forming galaxies (e.g., Hodge et al. 2013). These groups (separated by ~10-30" on the sky) represent ideal targets for a multi-object IFU such as GIRMOS to map their kinematics internally, with many having bright, compact starburst cores (<0.2″) requiring the highest resolution mode of GIRMOS. Using GIRMOS, we would aim to provide a statistical test to the triggering mechanisms of DSFGs by studying the Hα/[NII] dynamics of these starburst groups with ~1 kpc spatial resolution, which is crucial at at z~2, in distinguishing mergers and orderly rotating disks (Goncalves et al. 2010).

These observations will allow us to assess:

1. What triggers the intense star formation in bright DSFGs? Resolved Hα, [NII] velocity and dispersion maps trace star formation and dynamics of the galaxies? We will search for evidence of multiple dynamical components and asymmetry, which imply ongoing mergers.

2. Is there a metallicity gradient within the DSFGs? The gas phase metallicity (traced by [NII]/ Hα ratio) reflects past star-forming activity and the history of both gas inflow and outflow. Secularly evolving disk galaxies that follow inside-out growth tend to have initially steep negative abundance gradients, meaning high (low) metallicity at the centre (outskirts), which then flatten at later times (e.g., Gibson et al. 2013). However, mergers tend to rapidly flatten existing metallicity gradients by inducing an inflow of metal-poor gas to their central regions (e.g., Rupke et al. 2010).

3. Do most DSFGs have strong outflows and are they driven by AGN or star formation? With high SFRs and 30% containing AGN (Alexander et al. 2005), bright DSFGs are expected to be experiencing strong radiation/thermal feedback, which drives kpc-scale outflows that eventually enrich the circumgalactic medium. Strong outflows are traced through broad spectral emission (FWHM ~1000 km/s) and/or high velocity offsets from the systematic redshifts at >500km/s.

Overall GIRMOS observations will provide the definitive measure of the triggering mechanisms and processes that sustain the incredibly high star formation rates of DSFGs from the of peak epoch of galaxy formation at z~2 to the earliest times these luminous galaxies are found at z~7. The resolved nebular line properties will enable an understanding of the duty cycle of luminous bursts, and will serve as essential input to galaxy formation models, which presently struggle to produce realistic ultra-luminous galaxies at early epochs.

6.3.3.1. Observational Requirements

Our goal is to observe the measure the internal kinematics of DSFGs at early epochs using the nebular lines available in the J,H,K bands at each redshift range.

Using GIRMOS in the 0.1" sampling AO mode (corresponding to an angular resolution of 0.8 kpc at z ~ 1), we will observe 100 galaxies, with typically one DSFG per GIRMOS pointing, the remaining 3 GIRMOS arms targeting less luminous galaxies in the same fields (the targets of other programs).

We require a rest-frame velocity resolution of ~ 25 km/s for galaxies at z~2.5 and H-alpha at ~2300 nm which can be achieved with an R = 6000 grating. In order to measure the resolved kinematics of the galaxies we baseline our observations to require an integrated S/N = 50 for each galaxy. We note that the quality of the kinematic measurements will vary based on the spatial distribution H-alpha, however that cannot be well-determined prior to observation and therefore baseline to S/N = 50 integrated.

Typical z > 2 DSFGs have integrated Hα flux ~ 2–10 x10-16 erg s-1 cm-2, angular extent of 1–2" and line widths of ~500 km s-1. Our previous NIFS-without-AO IFU observations (Alaghband-Zadeh et al. 2012) show that ~4 hr integration is required to reach this surface brightness at the 5σ level (3x10-16 erg s-1 cm-2 arcsec-2) in a ~100 mas IFU resolution element. We can thus centroid emission lines in each spatial pixel to within 5–10 km s-1, and measure the line flux to within 10% (this flux corresponds to a SFR of ~2 M⊙/yr). The success of this approach is demonstrated in Fig. 9 for ALMA-identified DSFGs observed in our VLT programs.

For our longest pointing we then require 12.5 hours of observations, and for the shortest we require 2.7 hours. The average will be 7.5 hours per GIRMOS pointing, and 100 pointings requires 750 hours of observations, but multiplexed with other programs, effectively requiring 175 hours total.

6.3.3.2. Specific case study of a multiple DSFG system suitable for GIRMOS

While typically DSFGs are too rare to allow for use of the multiplexing capability of GIRMOS, in rare specific cases, there are clustered configurations of DSFGs, with suitable tip-tilt stars, that GIRMOS would be ideal for.

As an example, the most luminous HyLIRGs in the Universe: Panchromatic observations of the best candidate hyper-luminous infrared galaxies from the widest Herschel extragalactic imaging survey have led to the discovery of at least four intrinsically luminous z=2.41 galaxies across an 30" (240 kpc) region - a cluster of extreme starbursting proto-ellipticals (Ivison et al. 2013). Via subarcsecond interferometric imaging in the millimetre, accurate gas and star formation surface densities have been measured. The two brightest galaxies have extents of about 0.5" (4 kpc) FWHM in submillimeter/radio continuum and CO4-3, and possibly double that in CO1-0. The broad CO lines of these brighter two members due to large rotational velocities in counter-rotating molecular gas disks -- a scenario predicted to lead to the most intense starbursts, which will therefore come in pairs. The disks have M(dyn) of several 1011 M_ and gas

fractions of ~40%. Velocity dispersions are modest so the disks are unstable, potentially on scales commensurate with their radii: these galaxies are undergoing extreme bursts of star formation, not confined to their nuclei, at close to the Eddington limit. Their specific star formation rates place them 5x above the main sequence, which supposedly comprises large gas disks like these. Their high star formation efficiencies are difficult to reconcile with a simple volumetric star formation law. N-body and dark matter simulations suggest that this system is the progenitor of a Binary-type 1014.6 solar mass cluster.

6.3.4. Observations of Distant Galaxy clusters and groups: Observing Galaxy Quenching and the role of Environment at Early Times

Understanding the processes by which galaxies quench their star formation remains one of the most significant outstanding components in our best models of galaxy formation. Major studies in the last decade (e.g., Peng et al. 2010; Muzzin et al. 2012; Wetzel et al. 2013) have indicated that the physical processes causing quenching can be divided into two broad categories, one due to secular processes most likely related to the mass of galaxies (mass-quenching) and processes related to the environment of galaxies (environmental quenching).

There is mounting evidence from studies of the local universe that the physical process most likely responsible for environmental quenching is gas stripping. Ram-pressure from motion through the intra-cluster medium (ICM) can remove substantial amounts of gas from a galaxy and potentially quench it on the order of the dynamical time of the halo (~ 1 - 2 Gyr). Figure 11 shows an example of this, VLT/MUSE H-alpha observations of the galaxy ESO137-001 at z = 0 falling into the Norma cluster (Fumagalli et al. 2014). Remarkably, a trail of hot gas covering > 30 kpc is observed being stripped from the galaxy. The kinematics (color coding) show that the rotation within the galaxy is seen in the tail during the stripping process, and that additional star-formation events are also occurring in the tail.

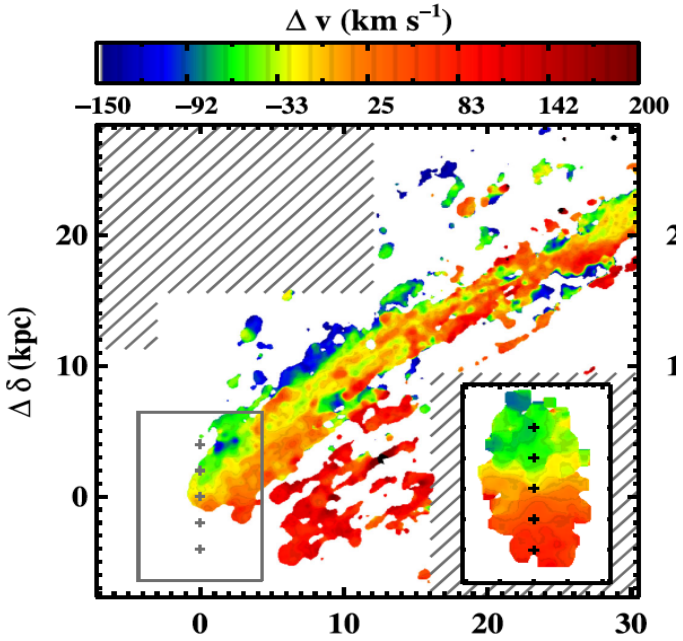

Figure 11: MUSE H-alpha observation of gas in the ram-pressure stripped galaxy ESO137-091 at z = 0 from Fumagalli et al. (2014). GIRMOS will make similar observations of galaxies at z > 1

Ram pressure stripping (RPS) events such as these are just starting to be studied in large numbers in the nearby universe by IFU surveys with MUSE (e.g., VESTIGE; Fossati et al. 2018, GASP; Poggianti et al. 2018). While at this point it seems reasonable to implicate RPS as the dominant cause of environmental quenching, we have precious little information on how the process works. For example, the vast majority of galaxies in clusters and groups quenched ~5 - 10 Gyr in the past (e.g., Smith et al. 2012) when clusters were far less evolved and galaxies had much higher gas fractions. Is the RPS we see in the Virgo cluster really analogous to the RPS that quenched the majority of cluster galaxies at $0.5 < z < 1.5$? Given the different conditions at high-redshift this seems extremely unlikely, and therefore if we wish to understand how the majority of galaxies quench, we need to observe RPS in the most distant clusters and groups.

At present, very few resolved imaging studies of the gas in cluster galaxies at $z \sim 1$ have been performed. Figure 12 shows preliminary results of HST/WFC3 G141-grism observations of star-forming galaxies in $z \sim 1$ clusters from Matharu in-prep. These images show the first evidence that the star-forming disks of cluster galaxies are smaller than those of non-cluster galaxies. While it is remarkable to see what appear to be ram-pressure stripped disks in the early universe, the S/N of the HST observations is low, the angular resolution is poor, and much more

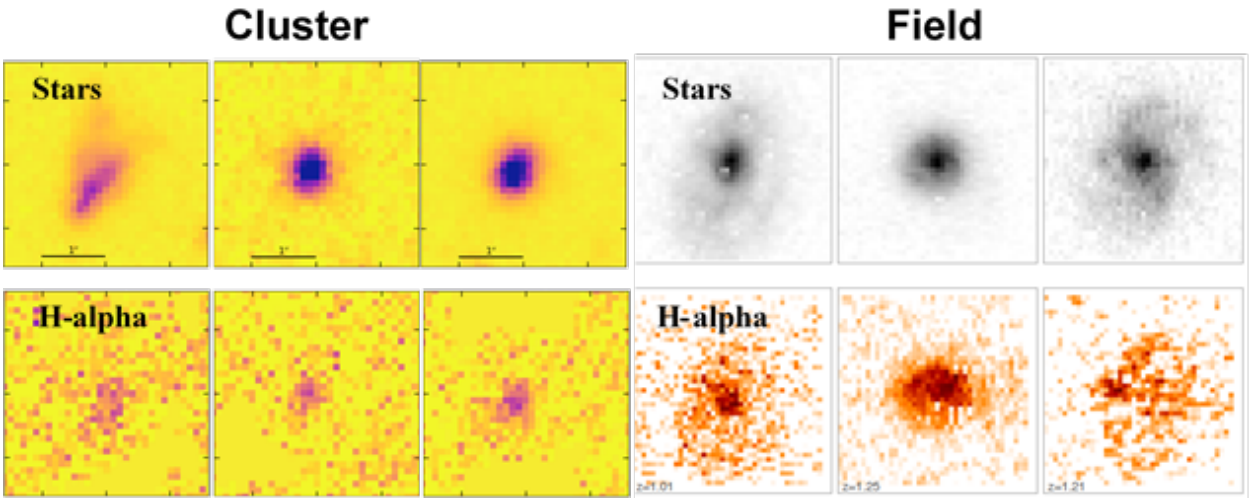

Figure 12: Left panels: Hubble Space Telescope observations of star-forming galaxies in clusters at z = 1. The top panels show stellar continuum imaging, the bottom panels show imaging at the wavelength of H-alpha (Matharu in prep). Right panels: Same as right panel but for galaxies in the field drawn from the 3DHST survey (Nelson et al. 2016). Galaxies in the field have star-forming disks slightly larger than their stellar disks. Galaxies in clusters have much smaller H-alpha disks, which is mostly likely due to ram-pressure stripping. GIRMOS will be able to produce similar such maps at higher spatial and spectral resolution as well as higher S/N, and will be essential for understanding how ram-pressure stripping works at z > 1.

information is needed to truly understand the process. With its AO IFU capability and multiplexing, GIRMOS will be the state-of-the art instrument to observe the H-alpha line at < 1 kpc spatial resolution in distant clusters. Our team will observe a sample of 80 star-forming cluster and group galaxies at z ~ 1. These observations will allows us to:

1. Measure the H-alpha sizes and light profiles with better than 1 kpc angular resolution and better S/N than the WFC3 grism, and provide the first unequivocal evidence for environmental quenching when the universe was only 3 - 4 Gyr old
2. Measure the kinematics of galaxies being quenched and how they depends on clustercentric radius and galaxy mass. Do higher mass galaxies experience weaker RPS? How does RPS proceed in more gas-rich galaxies?
3. Measure star formation gradients in quenching galaxies. Do galaxies quenching inside-out, outside-in? Does ram-pressure enhance the star-formation of galaxies before it quenches them? Does it alter the morphology of galaxies?

Overall GIRMOS observations will provide the definitive measure of the effects of environment on galaxies at the peak epoch of environmental quenching and will serve as essential input to galaxy formation models, which presently struggle to produce realistic cluster galaxies.

6.3.4.1.Observational Requirements

Our goal is to observe the measure the internal kinematics of star-forming galaxies in clusters to ascertain if environmental quenching processes have altered the kinematic structure of galaxies. Using GIRMOS in the 0.1" sampling AO mode (corresponding to an angular resolution of 0.8 kpc at z ~ 1), we will observe 10 clusters with 4 - 12 galaxies in each for a total sample of 80 galaxies.

We require a rest-frame velocity resolution of ~ 25 km/s for galaxies at z ~ 1 and H-alpha at ~1300 nm which can be achieved with an R = 6000 grating. In order to measure the resolved kinematics of the galaxies we baseline our observations to require an integrated S/N = 50 for each galaxy. We note that the quality of the kinematic measurements will vary based on the spatial distribution H-alpha, however that cannot be well-determined prior to observation and therefore baseline to S/N = 50 integrated.

Our targets have in-hand H-alpha flux from WFC3-G141 grism observations, which allows us to carefully tune the exposure time. The H-alpha fluxes range from $5e^{-18}$ erg s^{-1} cm^{-2} to $5e^{-16}$ erg s^{-1} cm^{-2} and therefore require on-sky integration times of 1 - 10 hours to reach an integrated S/N of 50 for each galaxy.

For our longest pointing we then require 12.5 hours of observations, and for the shortest we require 2.7 hours. The average will be 7.5 hours per GIRMOS pointing, and 20 pointing requires 150 hours of observations.

6.3.5. A Survey of Distant Quiescent Galaxies

The mechanism by which massive galaxies shut down star formation is a point of contention in galaxy evolution studies. Multiple processes have been proposed, including active galactic nuclei feedback, shock heating, gas starvation and depletion, and many others (Man & Belli 2018, and references therein). Understanding the cosmological context and physical properties of distant quiescent galaxies is fundamental to constrain their quenching mechanisms, and to inform how they evolve into the cores of present-day giant elliptical galaxies.

The quiescent nature of these distant galaxies makes them very challenging to observe. Their evolved stellar populations imply that their spectra are dominated by A-stars, since the younger O- and B-stars have died off. Deep, near-infrared spectroscopy is needed to obtain age and star formation history constraints, by means of detecting absorption features at rest-frame optical wavelengths, such as the Balmer series or Fraunhofer lines redward of ~3900 Angstrom. The brightest, most massive quiescent galaxies at z~2 are faint (K_AB ~ 20; e.g., Toft et al. 2012, van de Sande et al. 2013), requiring several hours even with 8 to 10-meter class telescopes to obtain sufficiently deep spectra for absorption line studies. Several surveys with the VLT, Keck and Gemini have confirmed their quiescent star formation rates, high stellar masses and evolved stellar ages, as well as high velocity dispersions of up to several hundreds of km/s. Their star formation history requires that quenching takes place rapidly, on the order of 100 Myr (Belli et al. 2018).

Faint emission lines such as [O III], [N II] and [S II] have been detected in these distant quiescent galaxies (Kriek et al. 2009, Newman et al. 2018a), although it is unclear if they originate from faint AGN, AGB stars or shocks.

A further complication is that quiescent galaxies are too compact to be resolved by the natural seeing. Their average half-light radius is 2 kpc or less, corresponding to less than 0.3" at z=1-3 (Newman et al. 2012, van der Wel et al. 2014). HST deep field imaging surveys provided the first evidence that quiescent galaxies are increasingly disk-dominated at earlier cosmic epochs (Chang et al. 2013). More recent studies of a few gravitationally magnified, distant quiescent galaxies have revealed that their stellar kinematics can have significant rotation (Toft et al. 2017, Newman et al. 2018b). The implication of these findings is that star formation quenching is not necessarily accompanied by structural transformation, seemingly at odds with predictions from the merger-triggered quasar feedback scenario (Hopkins et al. 2008).

To definitively conclude the mechanism responsible for quenching, we need a large sample of quiescent galaxies with spatially resolved spectra. The multiplex capability of GIRMOS will make it feasible to obtain a statistical sample of distant quiescent galaxies. While Keck/MOSFIRE also has multiplex capability and has been used to survey quiescent galaxies at z~2 current surveys (Belli et al. 2018), spectroscopic surveys to date are limited by the ground seeing and only provide integrated measurements. The JWST/NIRSpec is not expected to provide IFU spectra for statistical samples of quiescent galaxies because the IFU mode can only be operated on one object at a time.

We will take stock of GIRMOS's multiplexing and AO capabilities to conduct a survey of quiescent galaxies at z=1-4, in order to:

- Map the spatial distribution of the faint emission lines to discern their physical origins.
- Resolve the stellar continuum to perform kinematic and stellar population gradient studies.
- Provide a field control sample to complement the cluster survey in disentangling environmental effects.

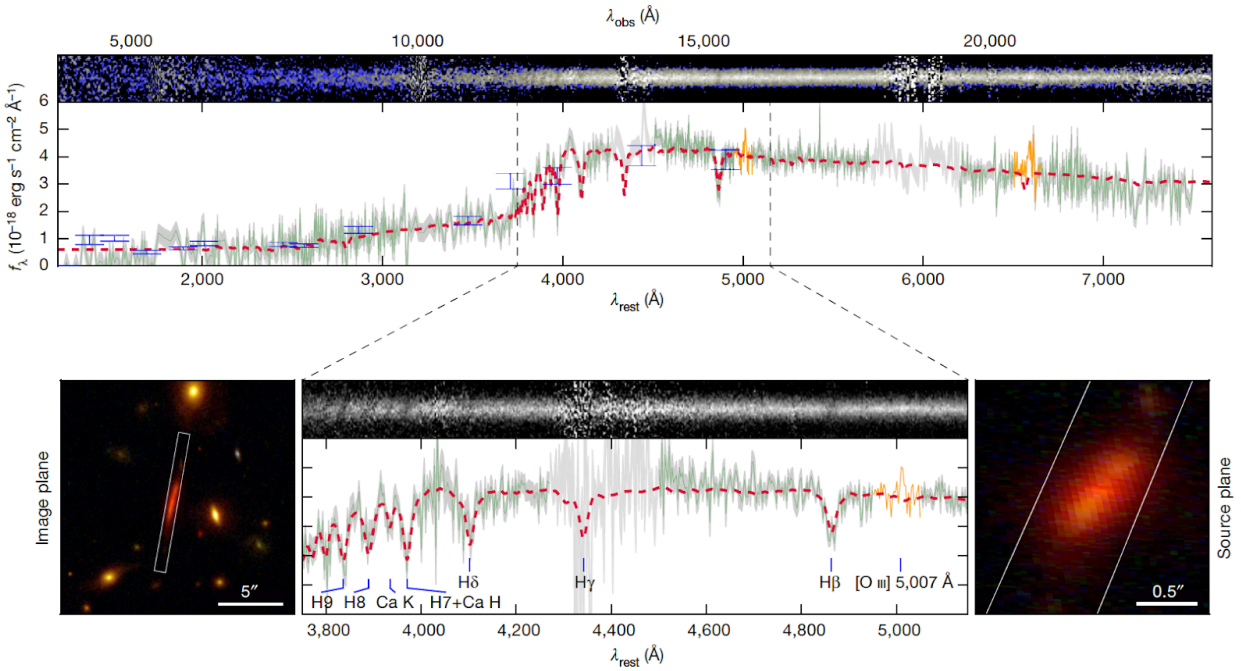

Figure 13: A VLT/X-SHOOTER spectrum of a z~2 lensed quiescent galaxy, along with the HST image showing its structure as it appears on the sky (left) and reconstructed through the lens model (right). GIRMOS will detect faint emission lines (like [O III], Halpha) as well as absorption lines useful for constraining their stellar populations and ionized gas conditions. Figure taken from Toft et al. 2017.

6.3.5.1.Observational Requirements

Spectral resolution:

The typical stellar velocity dispersions of distant massive, quiescent galaxies are about 150-500 km/s (e.g., Belli et al. 2017). In order to resolve the absorption lines with 5 velocity bins, a spectral resolution corresponding to ~ 30 km/s in the rest frame is required. This translates to a FWHM of ~ 4.2 Angstrom at 6000 Angstrom for a quiescent galaxy at z=2 or R~4255. This is sufficient to deblend emission lines near each other, e.g., the Halpha is bracketed by the [N II] doublet at wavelength difference of -15 and +20 Angstrom, respectively. This is also sufficient for detecting rotation in the stellar kinematics as their Vmax is on the order of 180-320 km/s (Newman et al. 2018b).

A higher spectral resolution would maximize the usable spectral range unaffected by skylines. However the tradeoff is that higher spectral resolution would lead to a noisier spectrum because the light is spreaded over more spectral pixels. So this science case would be optimally done with medium spectral resolution of several thousands.

Spectral band:

This science case requires observations in multiple filters to cover all the lines of interest. It will reduce exposure times by a factor of 2, if GIRMOS could simultaneously observe more than one filter (similar to the H+K mode of VLT/SINFONI).

Spatial resolution, IFU size and orientation:
The targets will have half-light radii of ~2 kpc or ~0.25". To resolve within the half-light radius with several elements, we require the PSF FWHM to be 0.1" at most after AO corrections. Gradient studies would benefit from having data points beyond the effective radius. Since the targets have a variety of surface brightness profiles, adaptive binning will be most suitable to optimize the S/N in galaxy outskirts. The sky background would likely dominate beyond a few half-light radii. Thus an IFU FoV of larger than 2"x2" should be ample for this science case, and will provide pixels for sky subtraction within the IFU. Their compactness also means that there is no need to rotate the IFUs.

The spatial sampling will be chosen to optimally sample the PSF.

IFU placement: Quiescent galaxies are quite rare. The source density of massive galaxies above stellar masses of 10^10.8 solar masses is about 2280 per sq. deg, as estimated from the UltraVISTA survey (Muzzin et al. 2013). For a patrol field of 2 sq. arcmin this means we expect ~1.3 quiescent galaxy on average, although the estimate might be higher given that quiescent galaxies are generally more clustered than being randomly projected on the sky.

A larger patrol field could increase the number of quiescent galaxies. Alternatively, this survey is best conducted in combination with field star-forming galaxies survey to optimize GIRMOS' multiplexing capability.

Sensitivity:
For emission line in distant quiescent galaxies, H-alpha and [O III] are generally fainter than [N II] (Newman et al. 2018a). Using the lensed quiescent galaxy MRG-M2129 as an example, the H-alpha line flux is (6.7 x 10^-18) erg cm^-2 s^-1 Ang^-1 after correcting for lensing. A sensitivity of (1.3 x 10^-19) erg cm^-2 s^-1 Ang^-1 is required to detect the emission line at S/N = 5 if it is uniformly distributed over 10 spectral pixels.

The stellar continuum should ideally be detected at S/N = 4 per pixel for robust stellar population fitting. To detect rotation in the stellar absorption lines, we require at least a S/N of 1 per Angstrom (observed frame) to estimate the velocity centroid correctly for a z~2 galaxy.

6.3.6. Intrinsically faint galaxies at Cosmic Noon and in the Epoch of Reionization: GIRMOS and lensing clusters

Key idea: use the power of gravitational lensing to allow GIRMOS to study intrinsically very faint objects and/or investigate distant objects on spatial scales equivalent to better than the 8-metre diffraction limit.

GIRMOS will have the ability to produce spatially-resolved spectral line maps of z>1 galaxies at scales (~0.5 kpc at z=1–3) that will be sufficiently fine to study kinematics and internal gradients in key properties (such as star formation, age, metallicity, etc.). However, unless severe spatial/spectral binning is accepted, the SNR limitations of an 8-metre telescope will limit such studies to the bright/massive end of the galaxy population. To study the faint galaxies that constitute the bulk of the galaxy population at high redshift and that are thought to be responsible for reionizing the Universe at z>7 we will either have to wait for a GIRMOS-like instrument on an ELT… or we can use GIRMOS and observe distant galaxies that are strongly amplified by the gravitational lensing of massive, intermediate-redshift galaxy clusters.

Using lensing clusters to study background galaxies has been a key science goal of large HST surveys such as the Hubble Frontier Fields (Lotz et al.) or CLASH (Coe at al.). It is routine to have several strongly-lensed z>1 galaxies per cluster and sources at z>6 are not uncommon (e.g., Coe et al. 2012).

The gravitational lensing provided by the cluster gives two key advantages over blank fields: (i) the total flux of the lensed galaxy is boosted, making it possible to observe intrinsically less luminous targets in reasonable amounts of telescope time, and (ii) lensing stretches the image allowing us to resolve scales (in the source plane) that are below the diffraction limit of an 8-metre telescope. These effects will let us reach intrinsically faint objects that dominate the galaxy population and/or to resolve galactic structure on sub-kpc scales.

In total, we can anticipate three distinct "science redshifts" for this type of observation: (1) galaxies at the z~2-4 peak of cosmic star formation; (2) galaxies in the Epoch of Reionization at z>7; and (3) (unlensed) galaxies in the foreground clusters themselves. The 3rd of these (cluster galaxies) is considered in detail elsewhere; the first two are described below.

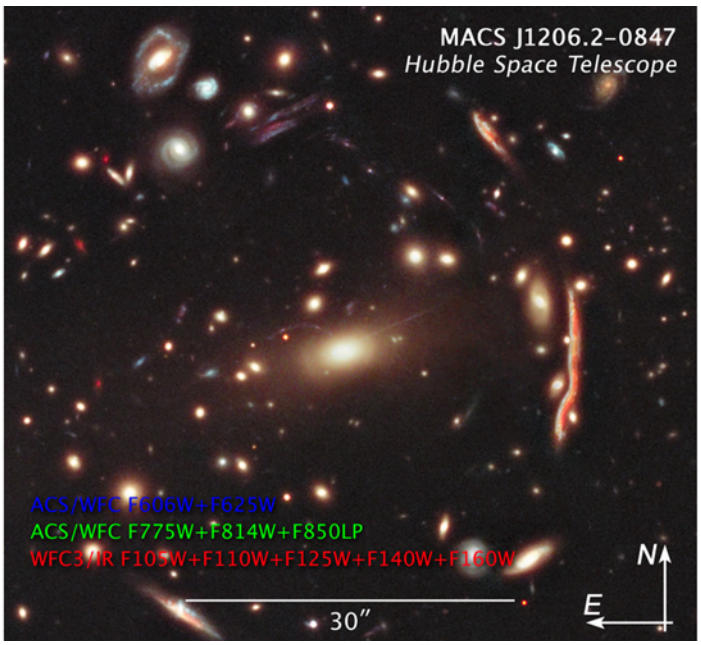

Figure 14: HST image of one of the CLASH survey lensing clusters. MACS J1206.2-0847. Multiple background lensed galaxies are apparent. Note the scale of the image, which is well-matched to the 2 arcmin GIRMOS patrol field

The projected size of the intermediate-redshift lensing clusters is well matched to the GIRMOS patrol field (see Figure 14) so that we should be able to place all 4 GIRMOS IFUs on lensed distant galaxies, or to place some of the IFUs on lensed galaxies and some on galaxies in the cluster. We can anticipate observing 2-4 z~2 galaxies per setting with perhaps two settings per cluster. Integration times are TBD but should be perhaps of order ~8-16 hrs per target. A survey of 20 lensing clusters, with a nominal two set-ups per cluster would thus take 40-80 nights and yield 20 lensed galaxies in the EoR, 40-60 lensed galaxies at z~2-4, and 20 (unlensed) cluster galaxies.

Science: At the peak epoch of cosmic star formation (z~2-4)

We anticipate that GIRMOS will be observing lensing clusters that have extensive HST data (and possibly JWST, including JWST NIRISS slitless spectroscopy — from, e.g., the NIRISS GTO program "CANUCS" which targets lensing clusters). Such data are essential for giving good lens models, but will also let us build spatially-resolved spectral energy distributions (SEDs) and (where NIRISS slitless grism data are also available) pre-select targets with promising line fluxes and spatial emission-line distributions. The SEDs will give us maps of stellar mass distribution in our lensed target galaxies to which we will add GIRMOS spatially-resolved emission-line maps and kinematic information. The kinematic information will let us tag our targets as rotationally-supported or otherwise, constrain their kinematic masses, and search for signatures of mergers and interactions. Instantaneous star formation rates will come from emission line fluxes (Hα, Hβ and [OII]), dust extinction from the hydrogen Balmer line ratios, and metallicities from the ratios of [OII], [NeIII], Hγ, Hβ and [OIII] lines. These measurements will be spatially resolved, revealing how these properties depend on the position within each galaxy. With these

data we will be able to measure the mass-metallicity relation — a key indicator of galaxy growth — for low-mass galaxies. At z~2 this is currently only known for high-mass systems, >109M⊙ (Erb et al. 2006; Steidel et al. 2014; Sanders et al. 2015) but the currently unknown low-mass end is of special interest because that is where the effects of star-formation-suppressing stellar feedback are expected to be the greatest. Spatially-resolved metallicities are important as this can provide information on prior star formation, outflows, gravitational infall and dynamical evolution in these galaxies. We will also measure the Hα luminosity function (a proxy for the SFR) and with the help of lensing we will detect galaxies with very low star formation rates (SFR~0.1—0.01M⊙/yr), a regime where the stochastic nature of star formation is important (Dominguez et al. 2015). We will then be able to determine how stochastic the star formation histories are by comparing UV and Hα luminosities and find where these low-mass galaxies lie on the SFR–stellar-mass main sequence and compare these with theoretical models.. Finally, if we observe in fields that will have been targeted by JWST NIRISS grism observations (with redshifts accurate to 1000 kms^{-1}) we will be able to investigate the environments of our GIRMOS targets (groups, clusters) and correlate their properties with these environments: e.g., we will investigate how the star-forming main sequence depends on whether galaxies are centrals or satellites (telling us about gas feeding mechanisms), or study the dependence of the stellar mass function on the position within the halo, testing environmental quenching models (e.g., Peng et al 2010) at high redshift.

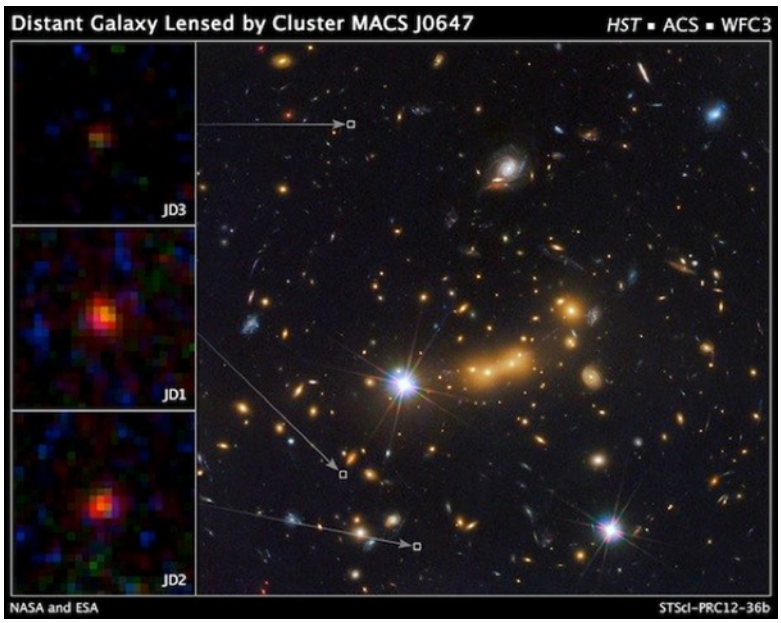

Figure 15: The z~11 galaxy candidate MACS J0647-JD located behind a z=0.591 lensing cluster (Coe et al, 2012). This is one of the highest-z galaxy candidates known. While this particular object is likely too faint for GIRMOS (it has not as yet been confirmed spectroscopically from the ground), other high-z sources are being discovered all the time.

Science: Into the Epoch of Reionization

The (re)ionization of intergalactic gas at z>6 is an important event in the early history of the Universe and is likely caused by the formation of stars in the very first galaxies. Tracing the decline in the relative strength of the Lyα emission line with increasing redshift, believed to be due to a higher neutral fraction in the intergalactic gas, gives us a way to monitor the reionization process (e.g., Schenker et al 2014, Konno et al 2014). Where possible, we will use GIRMOS to observe z>7 lensed galaxies pre-selected from JWST data (e.g., the slitless NIRISS GTO survey). With ~20 GIRMOS galaxies at z>7 we will study properties such as their kinematics and Lyα profiles. We will be able to compare our observations to reionization models to determine not only the global neutral gas fraction but also the patchiness of the reionization process.

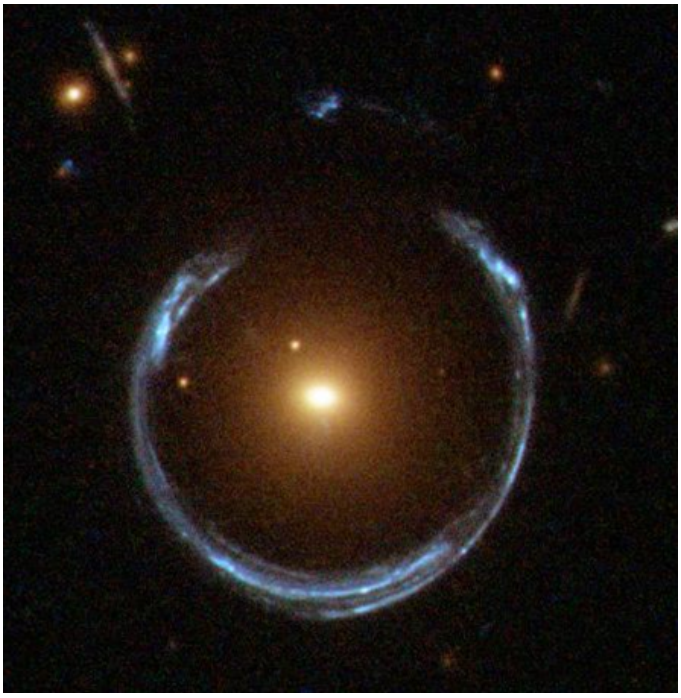

Figure 16: HST image of the Cosmic Horseshoe: a z=2.379 background galaxy in the LRG 3-757 lens system. The diameter of the lensed image is 10" (Belokurov et al. 2007, ApJ, 671, L9).

6.3.6.1. Observational Requirements:

The technical requirements are in many ways similar to those for other high-z galaxy studies planned for GIRMOS (though see further down for some key "extras"): R=3000 or 8000 (depending on source brightness) is needed to construct velocity maps. Lower resolution suffices for emission-line maps needed to construct SFR maps. Spatial resolution of <125mas is minimum, with <0.65mas desirable. Flux calibration and PSF measurement requirements are similar to those for other high-z science cases.

Because the number of viable targets per field is expected to be small (typically ~1-4 per lensing cluster), and because the sources can be expected to have different redshifts and brightnesses, it is desirable to have the individual IFUs be independently configurable (different R and wavelength settings allowable for each IFU).

Some gravitationally-lensed images will be relatively compact (<2") but some particularly interesting examples will be quite extended (up to ~10-15" — see examples in Figures 14 and 16), so it would be beneficial for observing efficiency to have buttable IFUs with the ability to configure up to 1x4 in a linear or even curved configuration.

6.3.7. Resolved Gas and Stars in Lyman Alpha Emitting Galaxies at z > 7

It is becoming increasingly clear that the earliest stages of galaxy formation play a defining role in their subsequent evolution. Theoretically, it is expected that the first galaxy-mass dark matter haloes collapse around $z \sim 100$ and that the first stars in galaxies start to form at $z \sim 10 - 20$. The universe becomes reionized at $6 < z < 10$ and at this epoch many galaxies are rapidly forming stars with specific star formation rates (SSFRs) as high as 6 - 24 Gyr^{-1} (e.g., Roberts-Borsani et al. 2016).

Given the observational challenges, the properties of galaxies at the epoch of reionization remains very poorly understood. At the time of this writing, only 13 galaxies at $z > 7$ have been spectroscopically-confirmed (Stark et al. 2017 and references therein). The majority of these have been with the detection of Lyman-alpha (hereafter LyA) in the Y-band, however some detections of the [CIII],CIII] doublet in the H-band have also been made (see Figure 17). JWST can access wavelengths up to 5μm and therefore will play

a significant role in studying this population in the rest-frame optical. However, there is

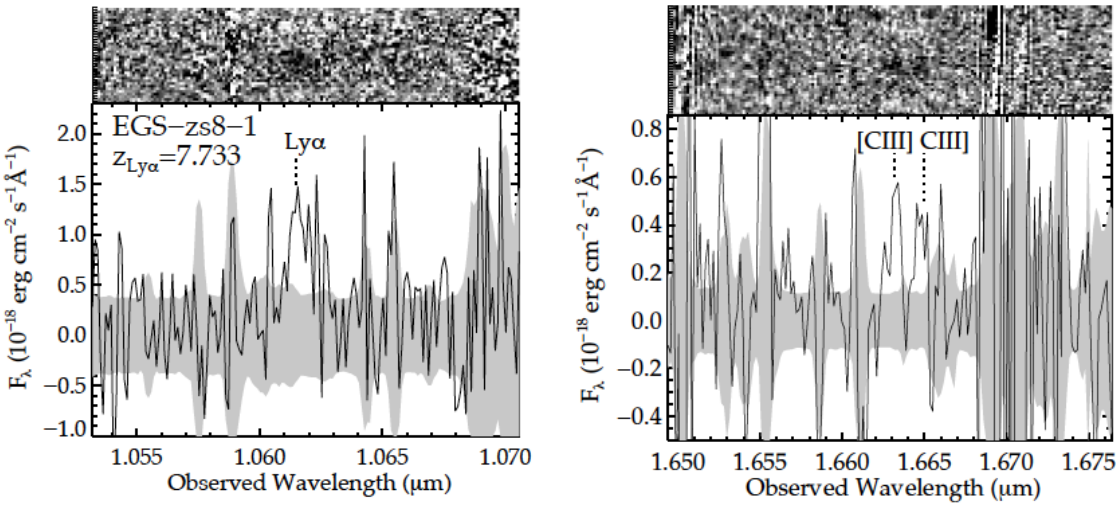

Figure 17: Left panel: MOSFIRE spectrum of the galaxy EGS-z8-1 at z=7.733 from Stark et al. (2017). The top panel shows the 2D spectrum which the bottom panel shows the 1D spectrum. Right Panel: Same as left panel but for the emission line doublet [CIII],CIII].

still much work in the rest-frame UV that can be done from the ground in the NIR. Figure 17 shows MOSFIRE spectra of EGS-z8-1, which is spectroscopically confirmed at z = 7.733 with both LyA and [CIII],CIII] emission in Stark et al. (2017). The expectation of the detection of galaxies at z > 7 with LyA emission is theoretically expected to be unlikely as this is in the epoch of reionization and it would be expected that neutral hydrogen will efficiently absorb LyA photons. Likewise [CIII],CIII] emission is expected to be faint. The detection of both in EGS-z8-1 suggests that an extremely powerful UV field may emanate from the galaxy, causing the enhanced [CIII],CIII] emission, and also blowing an ionization bubble large enough that LyA photons can escape. The authors measure a 360 km/s offset between [CIII],CIII] and LyA, with LyA redshifted, which is enough to allow it to pass through a non-ionized intergalactic medium and reach Earth. Precisely where the LyA originates from, and what its spatial distribution is remains an open question.

Figure 17 shows work by Hoag et al. (2019) who have attempted to model the spatial location of LyA emission for ~300 galaxies at 3 < z < 5.5 in the spatial direction of slit spectra in order to understand its spatial location. Theoretical arguments (e.g., Smith et al. 2019) suggest it may be extremely extended in size, much like the giant LyA "blobs" that have been discovered at lower redshift. Hoag et al. (2019) determined that on average the LyA emission comes from a region offset by 1.70 +/- 0.1 kpc from the centre of the galaxy, and that this offset decreases with increasing redshift. They speculate that if the offset continues to decrease, that z > 7 galaxies may have much higher than expected neutral hydrogen fractions in order to account for this decrease. Interestingly,

this contradicts the few spectroscopically confirmed galaxies at z > 7 such as EGS-z8-1, which in order to exhibit a high LyA and [CIII],CIII] EW which can only be explained with a low neutral hydrogen fraction! Clearly we still have much to learn about the intra galactic medium at these redshifts. As Hoag et al. (2019) point out in their abstract "Spatially-resolved observations of both LyA and UV continuum at 6 < z < 8 are needed to resolve this issue."

GIRMOS can play a significant role in providing the spatially-resolved LyA and UV continuum measurements required to understand the emerging intra-galactic medium for galaxies at the re-ionization epoch. Moreover they could also measure the kinematics of the gas, providing additional key information in modeling. Such observations would be expensive, with exposure times of 25 - 50 hours per galaxy required, however, if locations with multiple targets are located, the multiplexing of GIRMOS would still make this a feasible approach.

6.3.7.1. Observational Requirements

Wavelength coverage:
In order to observe the LyA line at z > 7, wavelength coverage into the Y-band is required. At z = 7 LyA is at 0.98 μm. If GIRMOS can observe as blue as 1μm, galaxies at z > 7.22 can be observed, which would be reasonable.

Spatial resolution & sensitivity:
Galaxies at z > 7 are generally extremely low-mass and compact (e.g., Mosleh et al. 2014, Bouwens et al. 2018), often smaller than 1 kpc. In order to spatially resolve these galaxies requires a spatial resolution < 1 kpc, or < 0.1" - 0.2" on the sky. So far only the brightest LyA emitters at z > 7 have been studied. The objects in Stark et al. (2017) have LyA fluxes ~ 5 - 10 x 10^{-18} erg s^{-1}. While faint, these can be detected in ~ 4 hours on-sky observations (for example the spectrum shown in Figure 16 is a 7.4σ detection in 4 hours on-sky integration from MOSFIRE). Spatially-resolved measurements require an integrated S/N = 30 which could be achieved with 8x longer integration, or 32 hours on-sky.

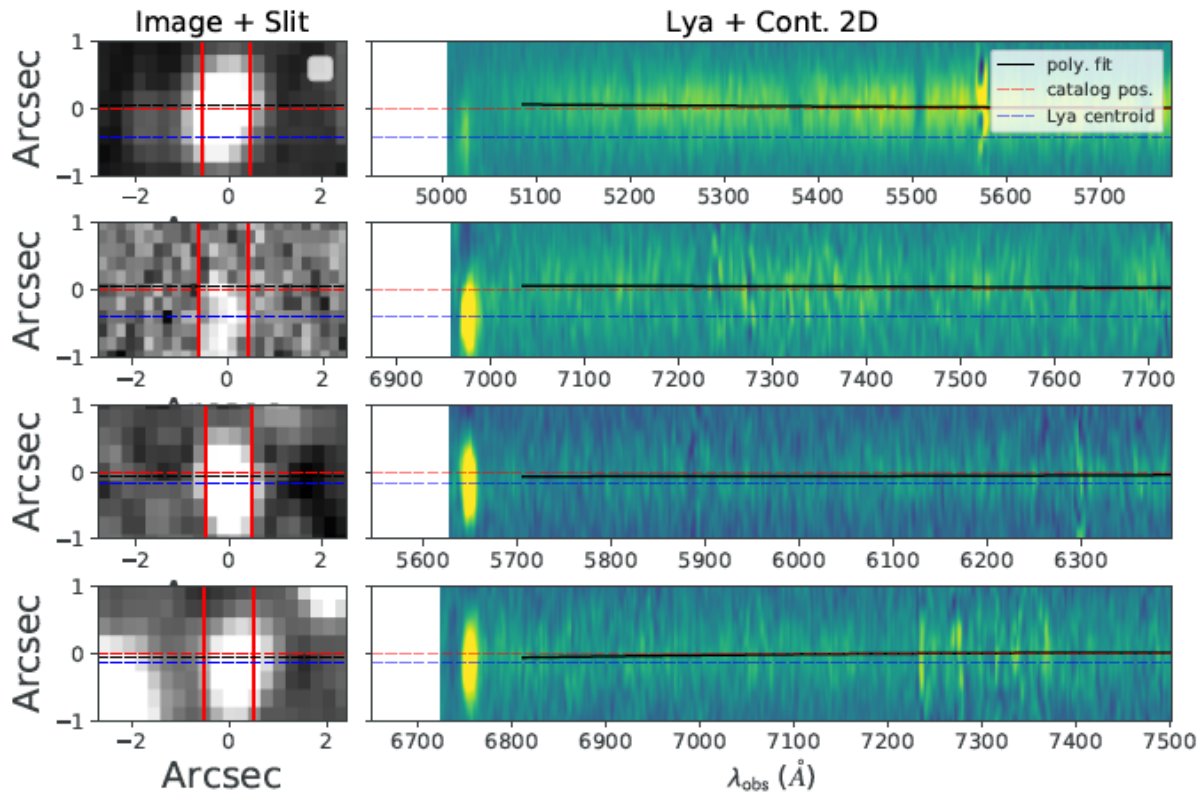

Figure 18: Left panels: Images of four galaxies at 3 < z < 5.5 from the VANDALS survey with the spectroscopic slit superposed. Right panels: 2D spectrum from the slit. In several galaxies an offset between the LyA continuum and UV continuum can be clearly measured. From Hoag et al. (2019).

6.4. Star-Formation

6.4.1. Young Star Clusters and Photo-dissociation Regions

Stars typically form in clustered environments within giant molecular clouds (Lada & Lada, 2003). With the onset of hydrogen burning, the radiative and mechanical feedback from new generations of stars is responsible for removing, heating, ionizing and photo-evaporating the surrounding natal molecular clouds (Krumholz et al., 2014). Eventually, these processes will expose the young star clusters, and we observe them in the optical regime as HII regions, i.e. bubble-shaped regions of ionized gas around young stars. The interface between the feedback-driving stars and the feedback-affected molecular clouds is the so-called photodissociation region (PDR, see Hollenbach et al., 1997 for a review), which is characterized by the transition from ionized to atomic, and from atomic to molecular gas (see Figure 18). Classical Galactic examples include the Orion Nebula, the Eagle Nebula and NGC 3603, with HII regions being observed throughout star-forming galaxies.

While the effect of feedback from young stars onto the surrounding molecular clouds is conceptually well understood, we are only now starting to be able to observationally

quantify said stellar feedback. This progress is primarily due to the rapid development of integral field spectrographs with increased spatial and spectral resolution (as well as better spatial and spectral coverage), which allow us to simultaneously study the feedback-driving stars and the feedback-driven gas. For example, recent VLT/MUSE observations of star-forming regions have led to the first observational quantification of how molecular clouds are being eroded by nearby young star clusters (McLeod et al., 2016), and how their massive stellar content regulates star formation (McLeod et al., 2018).

While showcasing the capability of IFUs to capture stellar feedback, these optical observations of exposed star clusters are not representative of the earlier stages of star formation. Indeed, observations show that young star clusters suffer from high infant mortality, with only about 4% of them surviving to become exposed clusters observable in the optical (Lada & Lada, 2003). It is also at these earlier, more embedded stages, that protostellar outflows, which are associated with both high- and in low-mass stars throughout star-forming regions, potentially play a significant feedback role due to the injection of momentum into the surrounding medium. Depending on whether star formation within molecular clouds is episodic or rather continuous, the combined momentum injection from protostellar jets and outflows can be enough to either unbind the native molecular cloud, or maintain a certain level of turbulence, stabilize the surrounding matter against gravitational collapse and therefore in regulating further star formation by slowing it down. Models of prostellar outflow feedback (Li & Nakamura 2006, Matzner 2007, Nakamura & Li 2007, Cunningham et al. 2009, Carroll et al. 2009) also show that because of the injected turbulence, outflows from low-mass stars can hinder high infall rates towards massive stars and therefore regulate the formation of these.

It is only with IR IFU instruments that we will be able to observe the still (partially) embedded young stars, study their effect on the surrounding matter, and understand their role in star cluster evolution. With its combination of AO-assisted high spatial resolution and the medium spectral resolution, GIRMOS will allow an unprecedented view on photodisscoiation regions in the Milky Way and the Magellanic Clouds. Of particular importance is the capability of simultaneously capturing both the ionized and the molecular gas (from the Brγ and ro-vibrational H2 lines in the K band, respectively) at high spatial resolution. GIRMOS will thus not only allow detailed spatially-resolved studies of the transition from the ionized to the molecular components in PDRs, but it will also allow to derive and analyze the gas kinematics and therefore derive feedback-related quantities. Moreover, we will be able to perform detailed analyses of outflows and jets from young stars (e.g. Figure 19), and therefore deliver a better understanding of their effect on their natal environment. At the same time, GIRMOS will enable to study young, partially embedded star clusters in great detail and perform spectral classification (e.g. Wallace & Hinkle, 1997) and hence directly relate the feedback-driving stars to the feedback-driven matter.

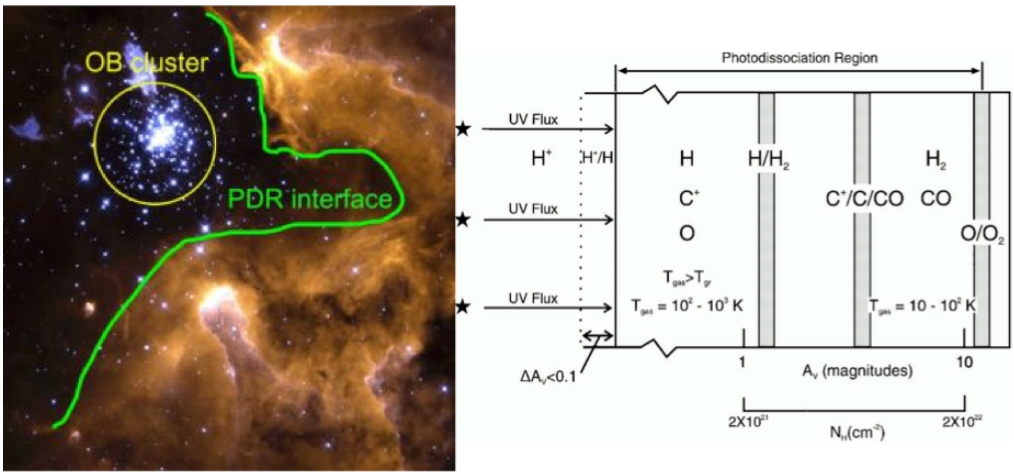

Figure 19: Left: HST image of the Galactic star-forming region NGC 3603 (Credit: JPL/IPAC, Univ. Washington Univ. Illinois Urbana-Champaign, and NASA), where a massive cluster of O- and B-type stars has formed an HII region. Shown in green is the photodissociation region where the ionized gas transitions to atomic and molecular gas. Right: a schematic view of a photodissociation region (adapted from Tielens, 2005).

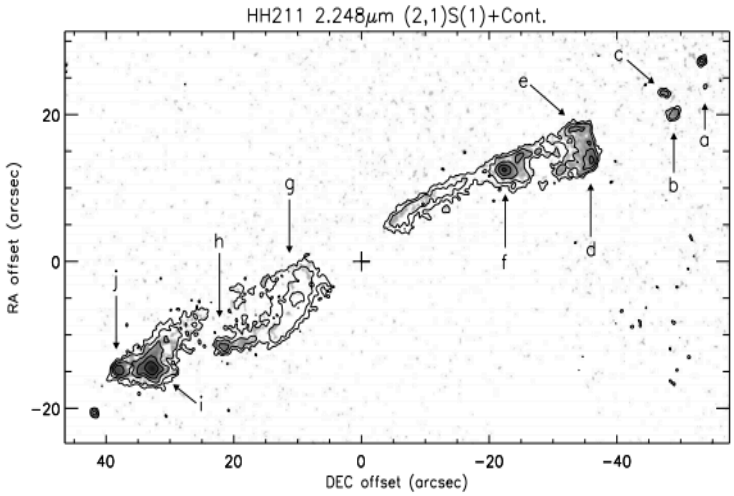

Figure 20: H2 (2-1) emission from the highly-collimated, jet-driven protostellar outflow HH 211 in Perseus (O'Connel et al., 2005).

6.4.1.1. Observational Requirements

Wavelength coverage:

The K band coverage of GIRMOS is of particular interest to study PDRs and protostellar jets/outflows, as it covers the Brγ line at 2.1655 μm as well as the main ro-vibrational transitions of molecular hydrogen (H2 (1-0) and H2 (2-1) lines at 2.122 μm and 2.248 μm, respectively). Additionally, the presence of several He I and He II lines is ideally suited to also classify massive stars, in addition to their lower-mass siblings.

Spatial resolution & sensitivity:
With a spatial resolution of the order of 0.05", we will be able to study PDRs, young star clusters and protostellar outflows on their relevant physical scales. At the distance of Orion (~ 420 pc), a spatial resolution of 0.05" corresponds to physical scales of about 20 AU, while at the distance of the LMC this would correspond to physical scales of about 2500 AU. This is ideally suited to perform the above-described studies, and hence drive significant progress in the field.
Despite the relatively small FOV, as an AO-assisted instrument with the capability of reaching sensitivities of the order of some 10-18 erg s-1 cm-2, GIRMOS will be superior to other ground-based NIR IFUs with comparable spectral resolution like e.g. KMOS on the VLT.

Spectral resolution:
With a K-band resolution of about 70 km/s, with the S/N ratios of the order of 30 or more, we expect to achieve a centroid velocity resolution of ~ 10 km/s, which is sufficient for the above-described science.

IFU placement:
The mosaic mode of GIRMOS will yield a FOV of ~ 10" x 10". While this is small compared to e.g. KMOS and a larger FOV would be preferable, when using it to efficiently map PDRs and perform targeted observations of star clusters, all the science goals will be met. For example, a ~ 6 x 4 = 24 pointing mosaic will cover the same FOV as one KMOS pointing, but at an order of magnitude higher angular resolution.

6.4.2. Young resolved massive star cluster formation and evolution

Although the formation of stars from a molecular clump is reasonably well understood this ignores the environment of the star formation process. Most stars are formed in clustered environments with a large fraction formed in clusters. Thus, in order to understand star formation we have to understand it in the context of star formation in clusters.

We have a reasonably good understanding of the end product of the star cluster formation. In older (more than 1 Myr) clusters where we can observe the individual stars in some detail since the molecular material out of which the stars have formed has been dispersed. However, at this point the star formation is mostly over and the clusters are already old, relative to their free fall time and all initial dynamical information is lost.

We are thus compelled to probe clusters while they are still forming stars. In particular we are interested in massive clusters since they both provide aims to study star formation in a very different environment than the low-mass, low-density environments near the sun. Their high density and the presence of massive stars which affects the environment through their high UV flux and strong winds provide conditions very different than those in low-mass environments.

Further, massive star clusters are probes into the distant Universe where they are the only sources that can be detected in the host Galaxy.

Despite their importance we know little about the formation of massive star clusters. Is their formation fast or slow? Both in terms of the free fall time and in terms of potentially multiple events spatially close that later merges. Does star formation on the scale of the formation of an individual star progress similarly to that in low-mass clusters? In other words, is the Initial Mass Function (IMF) the same in a low- and a high- mass star forming region? What is the fate of the forming massive clusters, will they remain bound or will they quickly disperse, thus becoming a major contributor of field stars over time?

Tackling these questions require both high spatial resolution as well as high sensitivity. Near-infrared observations are further necessary since the forming clusters are deeply embedded and, for the Galaxy, in the Galactic plane.

GIRMOS will be extremely well suited to address key issues. Through deep intermediate and high spectral resolution IFU observations stars in the pre-main sequence to main sequence transition can be targeted in the nearest massive young star forming clusters and complexes (e.g. NGC3603, and Westerlund 1/2 in the South and the W3/4/5 and W51 complexes in the north. With a spectral resolution of R=3000 the spectral type of the stars can be determined based on metallic lines. These sources can then be placed in the HR diagram for a direct comparison with stellar evolutionary models from where the object age can be deduced. For the "established" clusters like Westerlund 1 and NGC 3603 the final age spread can be deduced if the objects in the main sequence/pre-main sequence phase are targeted. For the younger complexes the individual sub-clusters can be targeted and the relative agree between them established.

The depth necessary to reach past the main sequence/pre-main sequence transition depends on the region observered, its age, distance and the extinction both along the line of sight and intrinsically in the star forming region. The younger the region the more massive the transition is but there is typically also more extinction in the region. As an example of the depth necessary to reach the science goals we use the observed characteristics of Westerlund 1, adopted from Brandner et al. 2008 (A&A, 478, 137). Figure 20 shows the photometrically derived color magnitude diagram for the intermediate mass of the cluster.

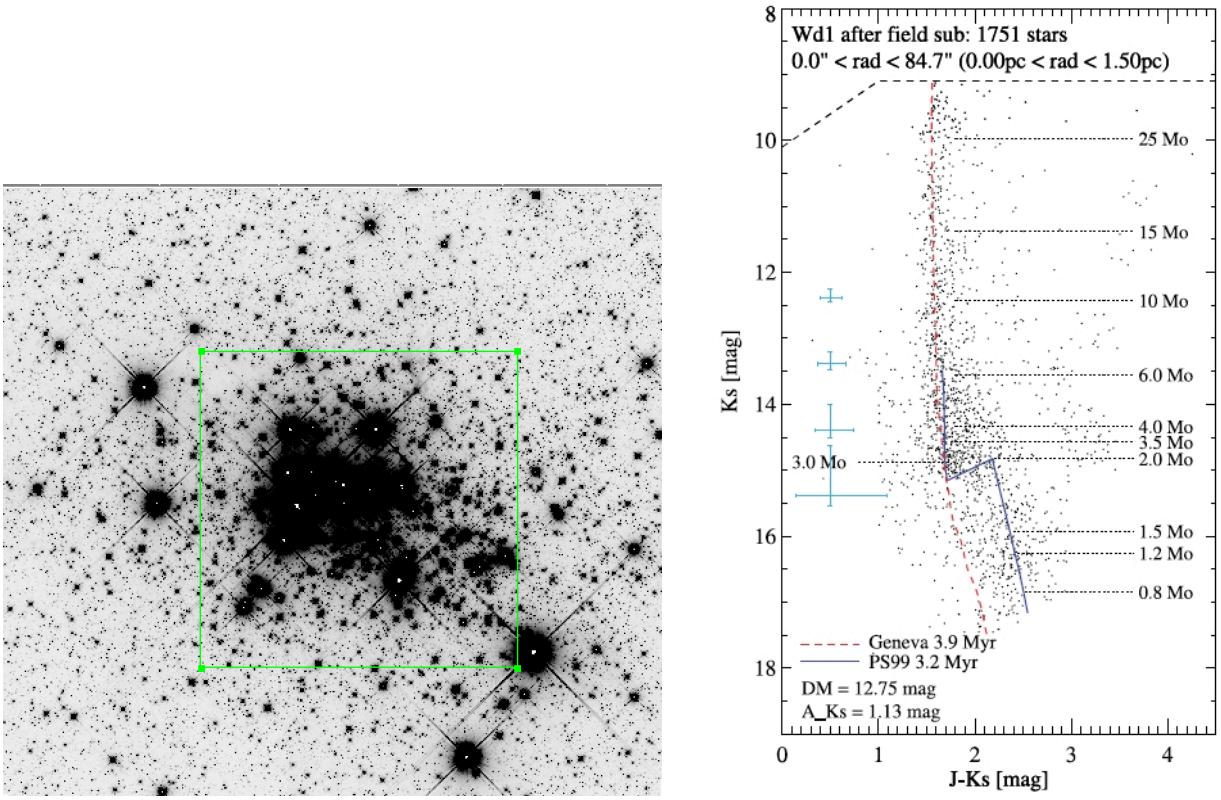

Figure 21: HST F125W image of Westerlund 1, with a 90" FOV shown as the green box. Right: Color-magnitude diagram for Westerlund 1 based on natural seeing near-infrared photometry (Brandner et al. 2008, A&A, 478, 137). The main sequence/pre-main sequence transition is seen at Ks~15mag. Spectral typing and accurate bolometric correction for these objects are necessary to accurately place the objects in the HR diagram and then determine the age distribution for the cluster.

With a spectral resolution of 8000-10000 it is possible to probe the intrinsic radial velocity distribution of a cluster. With high signal to noise the radial velocity can be determined down to a few km/s which is sufficient to determine if (sub)-clusters are gravitationally bound. Reaching the intermediate mass content is of importance since the clusters are expected to be mass segregated at a very early time. Thus, the radial velocities have to be determined for a range of stellar masses.

It is well known that the field population of intermediate mass stars show a high fraction of binarity. The same has been measured for the very massive content in a few massive young star clusters, e.g. 30 Dor and Westerlund 1. Thus we expect the binary fraction to be high as well for the intermediate mass content in massive clusters. Tight binaries will artificially enhance the measured radial velocity dispersion for single epoch observations and several epochs are needed to identify the binary stars. However, due to their short orbital period epochs separated by the time span of days and then a year are sufficient to correct the velocity dispersion (Cottaar et al. 2012, A&A, 547A, 35C, Cottaar & Henault-Brunet, 2014, A&A, 562A, 20C).

Galactic massive clusters are crowded and AO is crucial to obtain spectroscopy with as little as possible contamination from other sources and nebulosity. IFU observations are also of great importance to be able to accurately sample the local sky. Furthermore, a sample of stars are needed to be able to address the science topics described above. A sample of ~20-30 stars for each cluster will enable an analysis of the age spread and a similar sample is needed to derive the velocity dispersion.

6.5. Imaging of Transients and the Time domain

6.5.1. Broad-band photometric follow-up of multi-messenger events

A key driver for the Gemini observatories during the era of GIRMOS is the study of transient multi-messenger events, including kilonovae resulting from the mergers of binary neutron stars. Following the detection of the gravitational wave event GW170817, and its associated gamma ray burst GRB170817A that was detected 1.7 sec after the LIGO signal, we now know that at least some short-period GRBs result from such neutron star mergers. As of Fall 2021, GW170817 remains the only multi-messenger source that that been detected in gravitational waves (GWs) and electromagnetic radiation. However, rapid follow-up of short GRBs can provide information on the onset and evolution of kilonovae even when the associated GW signal goes undetected.

The optical and infrared emission from the merging of neutron stars has at least two distinct components: a standard afterglow, arising from the interaction of the relativistic jet with the surrounding medium (including material ejected in the formation of the neutron stars), and a kilonova component, powered by the decay of radioactive nuclei produced and ejected during the merger process. Thus, study of the GRB afterglow probes the jet structure and geometry as well as the properties of the surrounding environment, while study of the kilonova reveals the yield of heavy elements, including the lanthanides, actinides and precious metals such as platinum and gold. The kilonova component peaks in the near-infrared within days. In contrast, the afterglow is generally blue and peaks minutes after the explosion, but can take days to fade as it evolves towardsreddercolors.

As noted by Troja et al.(2019), the identification of the kilonova component can be challenging because of contamination from the underlying bright afterglow; in the particular case studied by those authors, the two components "required an uncommonly rich data set to be disentangled." The contamination of the kilonova light by the fading afterglow can affect the interpretation of the heavy element production. The properties of the afterglow depend critically on the orientation of the relativistic jet (e.g. Lamb & Kobayashi 2017), which depends on the geometry of the neutron star merger; this in turn is an essential ingredient for deriving the energetics of the kilonova, especially for cases where there are no orientation constraints available from a gravitational wave signal.

Thus, an "uncommonly rich," multi-wavelength dataset, probing the afterglow emission at early times, is critical for quantitatively modeling the evolution of kilonovae and understanding in detail the production of heavy elements.

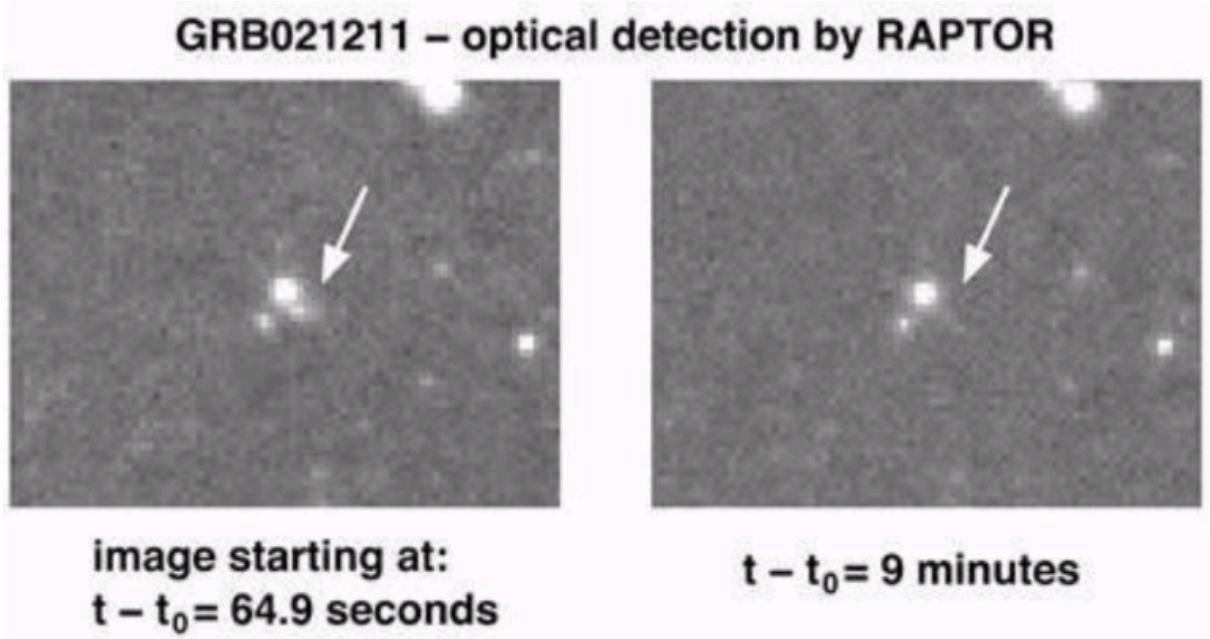

Figure 21: Example of a swiftly fading optical afterglow: the optical light associated with GRB021211 was clearly visible 65 seconds after the GRB trigger but had faded to the edge of detectability for the RAPTOR telescope after 9 minutes and was undetectable by large telescopes within a couple hours. Although many GRBs have lacked optical counterpart detection, it is likely that all events have some afterglow at optical or infrared wavelengths if observed early enough; if there is significant dust obscuration, the IR afterglow would be more easily detected. (Credit: Image taken by the RAPTOR telescope and RAPTOR team at Los Alamos National Laboratory. Copyright 2002 LANL and the University of California.)

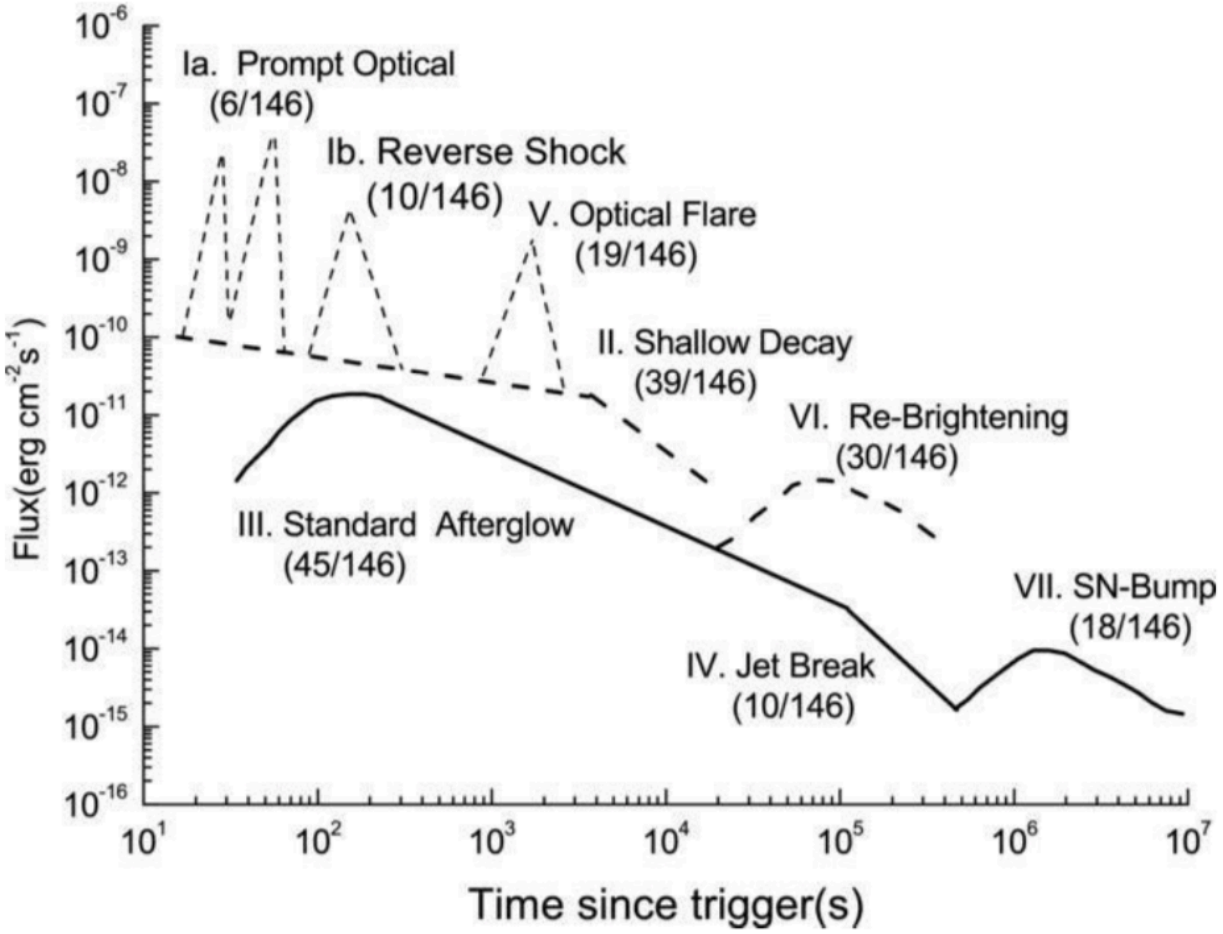

Figure 23: Schematic illustration of the various components that may occur in the light curves of the optical emission of either long or short GRBs; most GRB light curves will only show a minority of these components; the numbers in parentheses indicate the fractions of the GRBs exhibiting each of the components. The "standard afterglow" in the optical peaks within minutes of the trigger; for short GRBs (the ones associated with binary neutron star mergers), the "Re-Brightening" component could represent the kilonova, visible within hours (Li et al. 2012).

The question is, how early do we need observations? As illustrated in Figure 21, the evolution of the optical afterglow occurs quickly, perhaps fading several magnitudes on the time scale of minutes. Until recently, it was thought that many GRBs, especially short ones, did not have associated afterglows at optical and longer wavelengths; these were called "dark bursts." However, as localization becomes more rapid, it appears that even "dark bursts" have rapidly fading afterglows, and if these are followed to longer timescales, it may be possible to detect the onset of faint kilonova emission.

Figure 2 provides a schematic illustration of the various components that can contribute to the optical light curves of GRBs at early times. Kilonovae associated with short GRBs emit most of their light in the infrared; thus early observations at these wavelengths are particularly useful, and high-resolution, high-Strehl imaging, as provided by the GIRMOS imager using LTAO obserations, can minimize the contamination from the host galaxy

light. In order to get good constraints on the decline rate of the standard afterglow before the possible onset of a kilonova, observations should occur within about 1000 sec, or roughly 15 minutes, of the burst. Assuming it takes at least a minute to trigger the Gemini observations, and another four minutes to slew the telescope, the time to set up should ideally be no more than 10 minutes. Shorter acquisition times are desirable, of course.

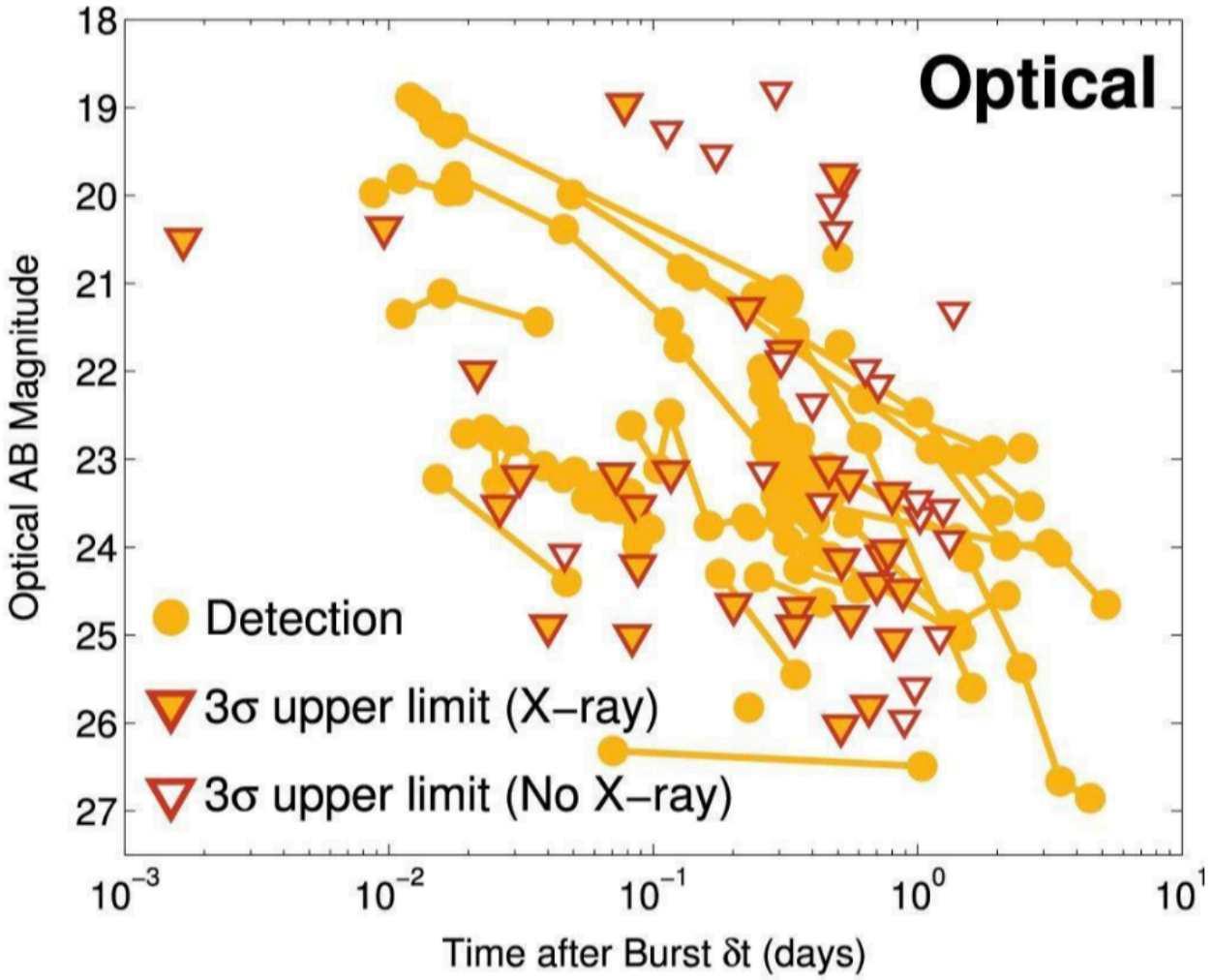

Figure 24: Broadband optical afterglow light curves of all 87 short duration GRBs (the type associated with binary neutron star mergers) with follow-up optical observations between 2004 November and 2015 March. Circles denote the 30 optical afterglow detections, triangles indicate 3σ upper limits, and solid lines connect observations for the same burst. Because the optical afterglows of short GRBs tend to be faint, only 10% of the optical detections were done with Swift's UV-Optical Telescope (UVOT) instrument, and 90% of the detections come from ground-based telescopes including Gemini. In contrast, for the brighter class of long GRBs, associated with the explosive deaths of massive stars, the majority of which have optical afterglows detected by UVOT within a minute of the burst. (Fong et al. 2015)

The main targets for multi-messenger follow-up studies in the near future will be associated with short duration GRBs. Because the optical/IR afterglows of short GRBs are generally fainter than those associated with long GRBs, relatively few short GRBs have

had early optical detections by *Swift*'s UV-Optical Telescope (UVOT). Instead, the follow-up has been done by ground-based telescopes; many of the photometric data points of relevance come from Gemini, Keck, VLT, and other large telescopes. However, none of the observations are from AO-assisted instruments; thus the GIRMOS imager would open a new high-resolution window for such studies. In order to be competitive in terms of time coverage, these observations should begin within $\sim 10^{-2}$ days, or about 14 minutes, again requiring an acquisition time of order 10 minutes (e.g., see Figure 2, which shows the broad band light curves of short GRB afterglows as discussed in Fong et al. 2015).

6.5.2. Synergies/complementarity with JWST, the Vera C. Rubin Observatory's LSST, the Nancy Grace Roman Space Telescope, and Euclid

The GIRMOS imager can provide critical observations that are highly complementary to JWST in the follow-up of MMA events. For the kilonova associated with GW170817, HST Target of Opportunity observations enabled important high-resolution photometric monitoring, particularly at IR wavelengths. However, because of restrictions in pointing and in the number of ToOs that can be accommodated on time scales less than the standard scheduling interval of two weeks, JWST will be much more limited in its ability to follow-up such events. Thus, GIRMOS can "fill the temporal gap" for kilonovae visible from Maunakea by providing high-resolution time-series photometric monitoring in the IR during the first two weeks after discovery. As the kilonova fades and becomes more difficult to observe against the bright ground-based IR sky background, JWST can target the source for longer term monitoring without the need to burn additional fuel because of unplanned slews.

Additional science gains can be obtained for transient observations that vary on short (minute) timescales, if fast (much less than 1 minute) read-out is possible. In this case, GIRMOS can be used to photometrically monitor transients for the purpose of obtaining a high cadence light curve (possibily corresponding to a kilonoae early in its decay, or some other unusual highly variable source). We also note that the entire field of view is not necessary to observe for most transients, and a single field of view will likely only ever contain a single transient event at a time.

6.5.3. Unknown unknowns in the time domain

When it becomes fully operational in a few years, LSST will provide an unprecedented view of the transient universe. With its deep survey range (r = 17 – 24 mag) and rapid cadence, LSST will produce orders of magnitude more transient sources than we can hope to follow-up with ground-based spectroscopic assets. Most classes of transients, including most common supernovae types, are readily classified from their light curves alone. The truly exciting opportunities in the time domain, as well as multi-messenger events discussed above, include the completely unexpected "unknown unknowns":

LSST will permit follow-up of rare and unexpected transients that will give us new insights into the physical processes at work in the extreme Universe.

We have a foretaste of the riches LSST promises in the results of on-going wide-field transient surveys designed to work at shallower depths (e.g., brighter than 16 – 17 mag) like Pan-STARRS, the All-Sky Automated Survey for Supernovae (ASAS-SN), Intermediate Palomar Transient Factory (iPTF), and the Catalina Real-Time Transient Survey (CRTS). While the photometric follow-up potential of GIRMOS is highlighted by consideration of kilonovae, discussed at length above, also important (especially for "unclassified" time domain events) is spectroscopic follow-up. Indeed, GIRMOS' ability to obtain both imaging and spectroscopy gives it a unique opportunity to become a premier facility for the rapid and sustained spectrophotometric monitoring of the evolution of transient sources using the queue-scheduled Gemini North telescope.

How this could work in practice is as follows. A new LSST transient event could trigger a ToO program in the Gemini queue. Gemini/GIRMOS slews to acquire and configure. An image, for example in K-band, is obtained, and then a probe arm is deployed and a broad-band spectrum is obtained. During this time, the imager also takes an image of the field surrounding the target. The probe arm is then removed from the target and a new science image obtained. This procedure can be repeated for as long as is desired. The images provide photometric datapoints as in the previous example with the kilonovae. However, the additional spectra provide new information of the time-evolution of the spectral energy distribution, which can be normalised to match the integrated flux from the source observed either side of the spectral observation. Indeed, the image taken during the spectral observation can also be used to correct for any changes in the atmospheric transmission during the spectral observation relative to the science photometry. In this way, GIRMOS can provide essential spectrophotometric data with which to classify and understand new transient phenomena.

6.5.3.1. Observational Requirements

- Given the need to track potentially fast-evolving transients, observations should be able to be executed within < 10 mins of starting program
- Fast (<< 1minute) read-out for high cadence photometric monitoring of transients that vary on minute timescales
- Broad band filter coverage, including at the bluest wavelengths which will overlap most with, for example, LSST discovery data. Consideration of LSST-like Y-band filter
- Sensitivities should be co-mensurate with other AO imaging instruments on 8m telescopes so GIRMOS is competitive in this field
- High photometric stability and accuracy required in order to track light curve over multiple nights. Calibratable to 1% night-to-night, and 5% overall zeropoint accuracy

- High astrometric accuracy in order to provide images with similar characteristics as IFU spectra. Choose similar precision, 10 mas (relative) and 300 mas (absolute)

8. Summary of Driving Science Parameters

The following matrix summarizes the driving science parameters, distilled from the Science Cases described above. These parameters represent the minimum instrument capabilities which are needed to achieve each of the science cases. A more detailed matrix can be found in Appendix A. The values contained in Table 1 are further translated into science requirements in the Design Requirements Document.

Table 1: Driving Spectroscopic Science Parameters

Observatory	Gemini					
Aperture	8 m					
Field of View	2' (GeMS FoV, ƒ/33)					
Spectrograph Type	Deployable multi-IFU					
Total Wavelength Coverage	1.0 µm - 2.4 µm					
Available Observing Modes	LTAO, MOAO, GLAO, Seeing-Limited					
PSF Estimation	Required					
Velocity Precision and Stability	1 km/s (relative), 20 km/s (absolute)					
Flux Precision and Stability	20% (absolute)					
Astrometric Precision and Stability	10 mas (relative), 300 mas (absolute)					
Observing Mode	LTAO/MCAO		MOAO		GLAO, Seeing-Limited	
Spatial Sampling Mode	High Res (11)		Med Res (1)		Low Res (9)	
IFU FoV	3.0" x 3.0" (11)		4.0" x 4.0" (1)	10"x10" (4)	3.0" x 3.0" (9)	
Spatial Resolution	50 x 50 mas (11)		100 x 100 mas (1)		400 x 400 mas (9)	
Minimum # of IFUs	1		20 (1)	1	1	
Spectral Resolution Mode	High Res	Low Res	High Res	Low Res	High Res	Low Res
Spectral Resolution	8000 (12)	3000 (13)	8000 (2)	3000 (1)	8000	3000 (9)
Instantaneous Wavelength Ranges	Js: 1194 - 1350 nm Hs: 1500 - 1706 nm Ks: 2110 - 2379 nm	YJ: 950 - 1367 nm JH: 1250 - 1800 nm HK: 1630 - 2350 nm	Js: 1194 - 1350 nm Hs: 1500 - 1706 nm Ks: 2110 - 2379 nm	YJ: 950 - 1367 nm JH: 1250 - 1800 nm HK: 1630 - 2350 nm	Js: 1194 - 1350 nm Hs: 1500 - 1706 nm Ks: 2110 - 2379 nm	YJ: 950 - 1367 nm JH: 1250 - 1800 nm HK: 1630 - 2350 nm
Sensitivity per spaxel (1 sigma, 1 hour) erg/s/cm^2/A	Js: UNDEF Hs: 5.7e-18 (11) Ks: 2e-20 (14)	YJ: UNDEF JH: 1.76e-18 (13) HK: 1.71e-18 (13)	Js: 5.2e-20 (7) Hs: 5.2e-20 (7) Ks: 5.2e-20 (7)	YJ: 5.2e-20 (7) JH: 5.2e-20 (7) HK: 5.2e20 (7)	Js: UNDEF Hs: UNDEF Ks: UNDEF	YJ: 2e-18 (9) JH: UNDEF HK: UNDEF
Note 1: Spatial resolution assumes it will require at least 2 spaxels to Nyquist sample the resolution element						

Table 2: Driving Imaging Science Parameters

Broad Band Imaging Sensitivity (Point Source, 5 sigma, 5 hours on-source integration time, [AB Mag])	Y: TBD mag, J: 25.1 mag, H:24.8 mag, K: 25.2 mag
Broad Band Filter Wavelength Requirements	Y: (0.97 – 1.07 μm) J: (1.17 – 1.33 μm) H: (1.49 – 1.78 μm) K: (2.03 – 2.37 μm) Y [LSST]: (0.93 – 1.10 μm)
Filter change time	< 1 min
Photometric accuracy/stability	1% (relative), 5% (absolute)
Astrometric accuracy/stability	10 mas (relative), 300 mas (absolute)

A. Summary of Observational Requirements

The observational requirements for each science case are tabulated in the following matrix. Individual science cases are listed along the left-hand column and observational requirements are listed along the top row.

Within each column of requirements, red boxes are used to illustrate the driving (worst-case) requirements. These observational requirements are documented as formal requirements in the Science Requirements Document [RD-01].

Doc Section	Science Program	Science Objectives	Observations	Per observation wavelength coverage	Spectral resolution for observation(s) in column D	Number of sources on the field	Minimum spatial resolution (Diffraction limit for J/H/K: 32/43/56 mas)	PSF estimation required?	Required IFU size (typical size of object)	Line / Continuum sensitivity (depending on the case)	SNR	On-source integration time (hours)	Velocity precision and stability timescale (relative/absolute/both)	Flux precision and stability time scale (relative/absolute/both)	Astrometric precision and stability timescale (in	Sample size of objects	Driving or Enabled Science case?	Additional Notes
	An AO-Assisted Field Galaxy Survey 0.7 < z < 2.7: Faint Galaxies (K > 19)	A combination of high-resolution AO-assisted IFS and multiplexing capabilities of GIRMOS provides an opportunity to observe the effects of accretion, mergers, and feedback processes on <1 kpc scale for statistical samples of star-forming galaxies in this redshift interval. Emission line velocity and velocity dispersion fields will quantify the importance of major and/or minor mergers for galaxy mass assembly. Maps of emission line ratios, providing radial distribution of metallicity gradients, will probe the contribution of galaxy interactions to their chemical evolution. Furthermore, the emission line maps will provide spatially resolved maps of AGN and star formation activity diagnostics (i.e., spatially resolved BPT diagrams). In combination with the identification of outflows (through additional emission line components with velocity offsets and large velocity dispersions), emission line maps will test the role of AGN and star-formation feedback in driving galaxy transformation from star-forming to quiescent stage.	AO assisted observations of statistical samples of field star-forming galaxies to measure spatially-resolved dynamical properites, metallicities, and AGN/star-formation activity using a range of emission lines - Hβ, [OIII], [NII], Hα, [SII]	J+H: 1.1-1.7 μm and K: 2-2.4 μm for covering four emission lines: Hβ, [OIII], Hα, [NII] in 1<z<1.6 and 2<z<2.5 range (maximum simultaneous coverage); J:1.1-1.35 μm and H+K: 1.7-2.4 μm for covering Hα in 0.7<z<1 and 1.3<z<2.7 range (maximum Hα coverage) and four emission lines: Hβ, [OIII], Hα, [NII] in 1.3<z<1.7 and 2.1<z<2.5 range	R=3000 (faint objects)	>20	125 mas as the minimum requirement (< 1 kpc), < 65 mas (< 0.5 kpc) target resolution.	yes	typical size (out to ~3Re) is 3-4"	line sensitivity: faintest sources 5.0e-18 erg cm^-2 s^-1 A^-1, brightest sources >5.0e-16 erg cm^-2 s^-1 A^-1	50 per spectral pixel integrated over the entire galaxy,	3-25 hours	Single line precision < 20 km/s across IFU. Multi-line precision < 100 km/s across IFU (minimum)	absolute, 20% accuracy	N/A	100	Driving	Arguably the main science driver for GIRMOS. Sensitivity, throughput and overheads/efficiency are important considerations.
	An AO-Assisted Field Galaxy Survey 0.7 < z < 2.7: Bright Galaxies (K < 19)	Science goals are similar to the faint galaxy survey. The bright galaxy survey will be objects at lower redshifts and higher SFRs. This project will use the high spectral resolution grating. This will achieve velocity resolution of ~ 50 km s-1 in the K-band and will resolve the turbulence scale in galaxies. This opens up many aspects of kinematic study.	AO assisted observations of statistical samples of field star-forming galaxies to measure spatially-resolved dynamical properties at high velocity and spatial resolution. Primary goal is to observe H-alpha as it is the brightest line.	J:1.1-1.35 μm and H+K: 1.7-2.4 μm for covering Hα in 0.7<z<1 and 1.3<z<2.7 range (maximum Hα coverage) and four emission lines: Hβ, [OIII], Hα, [NII] in 1.3<z<1.7 and 2.1<z<2.5 range	R=8000 (faint objects)	1-5	125 mas as the minimum requirement (< 1 kpc), < 65 mas (< 0.5 kpc) target resolution.	yes	typical size (out to ~3Re) is 3-4"	line sensitivity: faintest sources 5.0e-16 erg cm^-2 s^-1 A^-1	50 per spectral pixel integrated over the entire galaxy,	3-25 hours	Single line precision < 20 km/s across IFU. Multi-line precision < 100 km/s across IFU (minimum)	absolute, 20% accuracy	N/A	40	Driving	This is a key science driver, and a unique science niche for GIRMOS. Fields with appropriate guide stars and > 4 targets will not be everywhere but are available.
	Observations of Galaxies Mergers and Metallicities	Measure metallicities, SFR and AGN contributions from emission lines in close pairs of galaxies, or recently coalesced post-mergers	AO assisted observations could permit measurement of radially dependent changes in mergers. Without AO, global measurements would still be useful for comparison to low z. Ideally, pairs would have separations <80 kpc (10 " at z=1)	J+H: 1.1-1.7 μm and K: 2-2.4 μm for covering four emission lines: Hβ, [OIII], Hα, [NII] in 1<z<1.6 and 2<z<2.5 range (maximum simultaneous coverage); J:1.1-1.35 μm and H+K: 1.7-2.4 μm for covering Hα in 0.7<z<1 and 1.3<z<2.7 range (maximum Hα coverage) and four emission lines: Hβ, [OIII], Hα, [NII] in 1.3<z<1.7 and 2.1<z<2.5 range	R=3000	2-3. Fields would be specially sleected to have a close pair or triplet.	125 mas as the minimum requirement (< 1 kpc), < 65 mas (< 0.5 kpc) target resolution.	yes	Out to 2 Re (10-15kpc) would enable comparison with gradients done at low z. This corresponds to ~2" at z=1.	line sensitivity: faintest sources 5.0e-18 erg cm^-2 s^-1 A^-1, brightest sources >5.0e-16 erg cm^-2 s^-1 A^-1	50 per spectral pixel integrated over the entire galaxy,	3-25 hours	Single line precision < 20 km/s across IFU. Multi-line precision < 100 km/s across IFU (minimum)	absolute, 20% accuracy	N/A	50 pairs	Driving	Pairs should be selected to have masses and redshifts within the range of the field galaxy survey, so that the latter can be used as a control sample. Pairs need not be observed in same pointing, e.g. if separations are too small.
	Observations of Gravitationally Lensed Galaxies	Measure resolved kinematics, metallicities, SFRs, and ages (where possible) of background galaxies (z~1—7) lensed by intermediate-redshift (z~0.5) massive clusters. The science goals of this program are similar to other high-z z>1 GIRMOS science cases, but there are two key areas that are not possible with un-lensed galaxies that this science case permits: (1) very faint galaxies that would otherwise be too faint to observe will be reachable due to the lensing boost (flux boost of ~2-4x is typical but up to ~30x is known); and (2) brighter galaxies will be spatially "super-resolved" by the lensing, allowing us to probe their properties on much finer physical scales that will be possible with the same instrument for unlensed objects.	AO-assisted high spatial and spectral resolution observations of background galaxies (z~1—7) lensed by intermediate-redshift (z~0.5) clusters to characterize velocity fields or velocity dispersions, SFRs from emission lines, metallicities and ages from absorption lines/D4000. IFUs not allocated to lensed galaxies would be allocated to cluster or foreground or (not lensed) background galaxies, which in any case have similar technical requirements. Because of this, and because the lensed galaxies themselves will be at various redshifts, it is important that each IFU can be independently configured for resolution, wavelength coverage, and exposure time.	J: 1.1 - 1.35 μm, H: 1.5 - 1.7 μm, K: 1.99 - 2.4 μm	R = 3000 and R = 8000 depending on target brightness	typically ~1-4 per field, but some may benefit from cuttable IFUs	125 mas as the minimum requirement (< 1 kpc), < 65 mas (< 0.5 kpc) target resolution.	yes	2-10". Some objects may be quite extended (up to ~10"), so buttable IFUs would be a big boost for efficiency.	line sensitivity: faintest sources 5.0e-18 erg cm^-2 s^-1 A^-1, brightest sources >5.0e-16 erg cm^-2 s^-1 A^-1	50 per spectral pixel integrated over the entire galaxy,	4-20 hours	Single line precision < 20 km/s across IFU. Multi-line precision < 100 km/s across IFU (minimum)	absolute, 20% accuracy	N/A	20 clusters	Driving	This is a project where GIRMOS could be a world-beater: The multiplexing of several sources per cluster makes this more efficient than JWST or other ground-based AO-fed IFUs. The source density and FOV per cluster is well-matched to GIRMOS. More IFUs probably doesn't confer a huge advantage for strongly lensed galaxies except in some rare cases, but having more IFUs would allow cluster and foreground and (non-lensed) background galaxies to be studied simultaneously, thereby increasing overall efficiency.
	An AO-Assisted Survey of High-Redshift Clusters 0.7 < z < 2.7	Measure the kinematics, star formation rates, metallicities, stellar populations and structure of galaxies in clusters on < 500 pc scales. This dovetails with other science cases on "field" galaxies. The primary science goal is understanding how environment affects galaxy formation in its earliest stages.	AO-assisted high spectral- and spatial-resolution observations of galaxies in clusters to measure resolved dynamics, metallicities, SFRs, and stellar populations (e.g., D4000). The primary measurement is the H-alpha line (flux, centroid, asymmetry), however, other lines such as [OIII] and Hbeta are also useful targets. D4000 and continuum will be measured for brighter galaxies	J: 1.1 - 1.35 μm, H: 1.5 - 1.7 μm, K: 1.99 - 2.4 μm	R = 3000 and R = 8000 depending on target brightness	20 - 100	< 125 mas is the minumum requirement (< 1 kpc). However < 65 mas (< 0.5 kpc) would be target resolution.	yes	typical size of object 1 - 2". IFU minimum requirement 3", ideally 4" would allow on-IFU dithering for largest galaxies	line sensitivity: faintest sources 5.0e-18 erg cm^-2 s^-1 A^-1, brightest sources 5.0e-16 erg cm^-2 s^-1 A^-1	50 per spectral pixel integrated over the entire galaxy	4 - 20 hours depending on brightness	Single line precision < 20 km/s across IFU (minimum). Multi-line precision < 100 km/s across IFU (minimum)	absolute, 20% accuracy	N/A	100	Enabled	The source density of objects in clusters will be extremely high, and these will likel be a type of object where GIRMOS excels. More IFUs could also easily be exploited here. Recommendation is to study the feasibility of increasing the number of IFUs.
	A Survey of Dusty Star Forming Galaxies at z>2 (DSFGs / SMGs depending on your heritage)	Probe the kinematics, star formation rates, metallicities, stellar populations and structure within DSFGs on < 500 pc scales. This parallels with other science cases on less luminous galaxies in clusters and in the"field" galaxies. The primary science goal is understanding the triggering mechanisms and how high star formation rates are sustained in galaxy formation in both its earliest stages, and when it is rapidly building up its stellar populations.	AO-assisted high spatial-resolution observations of DSFGs to measure resolved dynamics, metallicities, SFRs, and stellar populations. The primary measurement depends on redshift, but entails nebular lines accessible, with a focus on line ratios sensitive to metallicity (Ha/NII, OIII/Hb, OII/NeIII).	J: 1.1 - 1.35 μm, H: 1.5 - 1.7 μm, K: 1.99 - 2.4 μm	R = 3000	1 source per field, unless in rare dense protoclusters (e.g. SPT2349-56), where 5-30 sources could be candidate GIRMOS targets	< 125 mas is the minumum requirement (< 1 kpc). However < 65 mas (< 0.5 kpc) would be target resolution.	yes	typical size of object 1 - 2". IFU minimum requirement 3", ideally 4" would allow on-IFU dithering for largest galaxies		can map velocity fields down to <3sigma line detections using nearest neighbour priors on line position / strength	4 - 20 hours depending on brightness	Single line precision < 20 km/s across IFU. Multi-line precision < 100 km/s across IFU (minimum)	absolute, 20% accuracy	N/A	100	Enabled	More IFUs could also easily be exploited for the SMG protocluster case.
	A Survey of Distant Quiescent Galaxies	Obtain a statistical sample of z>=2 quiescent galaxies with absorption line spectra. With well-characterized stellar populations and ISM conditions we can constrain how they shut down star formation and how the red sequence is built	Deep AO IFU observations to spatially resolve their (1) faint emission lines ([OII], [OIII], [NII] and Halpha, [SII]); (2) stellar continuum for kinematic and stellar population gradient studies.	J: 1.1 - 1.35 μm, H: 1.5 - 1.7 μm, K: 1.99 - 2.4 μm. If design permits, simultaneous multi-band observation (e.g. J+H; H+K would make it more time-efficient)	R = 3000 and R = 8000 depending on target brightness	1 - 3	< 100 mas	yes	typical size of <0.25". larger than 2"x2" is fine	line: 1.3e-19 erg cm^-2 s^-1 Ang^-1; continuum: down to K[AB] ~ 23	5	4 - 20 hours depending on brightness	Single line precision < 20 km/s across IFU. Multi-line precision < 100 km/s across IFU (minimum)	absolute, 20% accuracy	300 mas, no timescale constraint. For comparison with other data sets (e.g. HST)	100	Enabled	The targets are very faint (integrated magnitudes of K[AB] > 20.5) and rather rare on the sky. Recommendation: simultaneous observation of more than 1 filter (e.g. J+H, H+K) while meeting spectral resolution requirements
	Resolving Disk Growth at 2 Gyrs after the Big Bang	Measure the kinematics and star formation rates of galaxies at z=3-4. This is a poorly studied redshift regime for kinematic work because galaxies are very small. First results from a small number of galaxies suggest a steep rise in the rotation dominated fraction of galaxies between z~3 to z~2. These observations will test if this is real or an issue of poor resolution and low-number statistics.	AO-assisted high spectral an spatial resolution observations of star-forming galaxies at z=3-4 to measure intrinsic velocity dispersion and resolved dynamics	H: 1.5 - 1.7 μm, K: 1.99 - 2.4 μm	R = 3000 and R = 8000 depending on target brightness	10 - 20	<100 mas (<0.75 kpc) Science could be done for largest galaxies with 125mas but most galaxies will be smaller	yes	2". these galaxies are small ~0.5-1 kpc. 4" IFU would be possibly allow on-source dithering but this will be complicated for multiple targets	faintest sources 5.0e-18 erg cm^-2 s^-1 A^-1,	50 per spectral pixel integrated over the entire galaxy	4 - 20 hours depending on brightness	Single line precision < 20 km/s across IFU. Multi-line precision < 100 km/s across IFU (minimum)	absolute, 20% accuracy	N/A	25-50	Driving	In regards to the velocity precision. We will want to co-add data over time (e.g. deep observations can often be taken over multiple semsters). Relative shifts can be calibrated through skylines if need be so this is not of major concern.
	A Redshift Survey of z > 7 Galaxies	Measure the resolved kinematics, ionization parameters and metallicities of LyA emitting galaxies at z > 7.	AO-assisted high spectral an spatial resolution observations of galaxies at z > 7 to measure resolved LyA and [CIII] emission	Y: 1.0 - 1.1 μm, J: 1.1 - 1.35 μm	R = 3000	1	< 125 mas is the minumum requirement (< 1 kpc). However < 65 mas (< 0.5 kpc) would be target resolution.	yes	typical size of object 1". IFU minimum requirement 3"	brightest sources 5.0e-17 erg cm^-2 s^-1 A^-1, most will be fainter	50 per spectral pixel integrated over the entire galaxy	4 - 20 hours depending on brightness	Single line precision < 20 km/s across IFU. Multi-line precision < 100 km/s across IFU (minimum)	absolute, 20% accuracy	N/A	10	Possibly driving, this is next decade science	This is extremely exciting science to consider long term. Source density of objects currently is low, there are more handfuls of objets bright enough, and likely without bright guide stars. However, after JWST/EUCLID/WFIRST surveys there are likely to be many candidates with stars bright enough and this would be unique GIRMOS science. Requires Y-band though.
	The Central Regions of Nearby Starburst Galaxies	Obtain spectra of the central regions of starburst galaxies within distances of ~20 Mpc. Studies of emission and absorption lines will be used to chart the recent star forming history in time and space, including in the nucleus. Emission lines provide information about the most recent episodes of star formation, while absorption features proide insights into star formation during the past few hunred Myr. Both large star-forming complexes and the 'field' between these would be observed.	AO assisted IFU observations of the central ~kpc of star burst galaxies. For the nearest galaxies individual IFUs will be centered on distinct star-forming complexes. For more distant systems the IFUs will be assembled into a super IFU.	H: 1.5 - 1.8um (second overtone CO bands; [FeII] emission, and Bracket series emission lines; Ballick-Ramsey C2 band head). K: 1.9 - 2.4 um (first overtone CO bands; HeI emission, Brackett gamma; H2 emission). J: 1.1 - 1.4um (Pa beta and gamma emission).	R = 2000 - 3000.	1 - 10 star-forming complexes per galaxy	<100 mas @ H and K. This corresponds to a spatial resolution of a few parsecs for the nearest starburts (i.e. the core size of star clusters), and to a few tens of parsecs for the more distant systems (a tenth or so of the charavteristic size of giant star-forming complexes).	Not essential to map and characterize spectral features. However, is required to measure line fluxes that will yield absolute star formation rates. The PSF should be well enough known to yield fluxes with a 10% error.	1+ arcsec	K_AB = 20 - 22 mag/arcsec2	10 per spaxal	1 hour **ON SOURCE**. It will be necessary to nod off of the source every few hundred seconds to obtain reliable background sky measurements with the same total exposure time as the science target. The nod offsets will range from a few arcmin for the most distant galaxies in the sample to a few tens of arcmin for the closest sample members.	~10 km/sec in one complete observations (10% of the velocity dispersion in a moderate mass disk galaxy).	1 - 10%	N/A	50 galaxies in the field and Virgo cluster	Enabled	
	An AO-Assisted survey probing the inner regions of Galactic Bulge Globular Clusters	The central regions of globular clusters contain valuable information regarding the cluster's dynamical state, dark remnant population, and formation conditions. Knowing a cluster's central velocity dispersion is a key measurement in determining whether a cluster is dynamically old and if it has undergone core collapse, which in turn allows for a cluster's properties at formation to be inferred. Measuring how stellar kinematic properties vary with clustercentric distance also allows for the presence of stellar mass and intermediate mass black holes to be explored. Aditionally, constraints on the stellar chemistry of the cluster core can shed light on the links between chemistry and dynamics for the multiple populations often found in globular clusters.	AO assisted IFU observations of the inner cores of a large sample of bulge globular clusters.	H: 1.5 - 1.7 μm, K: 1.99 - 2.4 μm	R~8000	1 GC per field	56 mas @ H,K-band (diffraction limit of K-band)	No	1-3"	AB = 16.85, 16.47 (K and H, respectively)	35 SNR per resolution element (both K and H)	4 hours	Relative: 1 km/s (through multiple features), Absolute: N/A	N/A	Relative: 10 mas, Absolute: N/A	20-30 GCs	Driving	
	Stellar chemodynamics of the Galactic Centre: the nuclear cluster around the supermassive blackhole of the Milky Way	Reconstruct the chemodynamical model of the nuclear star cluster around the supermassive black hole at the center of our Galaxy.	Deep AO IFU observations of the nuclear star cluster in the Galactic Centre	K: 1.99 - 2.4 μm	R~8000	1	100 mas @ K-band	No	8x8"	AB = 16.85, 16.47 (K and H, respectively)	35 SNR per resolution element (both K and H)	20 hours	Relative: 1 km/s (through multiple features), Absolute: N/A	N/A	Relative: 10 mas, Absolute: N/A	1 Nuclear Star Cluster	Enabled	
	The formation of Galactic Massive Star Clusters	Obtaining spectra of the intermediate mass content of young massive star clusters in order to spectrally classify the stars and thus to determine age spreads within the cluster. Higher spectral resolution observations will be used to determine the velocity dispersion of the clusters and potential sub-clusters	AO IFU observations of a sample of stars in Northern massive star forming regions.	H: 1.5 - 1.7 μm, K: 1.99 - 2.4 μm	R~3000 R~8000-10000	dozens within a few	~80mas @K	In general no	point sources but there needs some room for sky (less than 1")	H=17, K=16 (R=3000)	10 SNR per resolution element	1 hour	Relative of a few km/s centroid, handful of lines	Not too important; 5%	N/A	Dozen objects per cluster	Enabled	